TU Delft

Delft University of Technology

Crevasse splay morphodynamics near a non-vegetated, ephemeral river terminus
Insights from process-based modelling

Li, Jiaguang; van der Vegt, Helena; Storms, Joep E.A.; Tooth, Stephen

DOI
10.1016/j.jhydrol.2023.129088

Publication date
2023

Document Version
Final published version

Published in
Journal of Hydrology

Citation (APA)
Li, J., van der Vegt, H., Storms, J. E. A., & Tooth, S. (2023). Crevasse splay morphodynamics near a non-vegetated, ephemeral river terminus: Insights from process-based modelling. *Journal of Hydrology*, *617*, Article 129088. https://doi.org/10.1016/j.jhydrol.2023.129088

Important note
To cite this publication, please use the final published version (if applicable).
Please check the document version above.

Copyright
Other than for strictly personal use, it is not permitted to download, forward or distribute the text or part of it, without the consent of the author(s) and/or copyright holder(s), unless the work is under an open content license such as Creative Commons.

Takedown policy
Please contact us and provide details if you believe this document breaches copyrights.
We will remove access to the work immediately and investigate your claim.

This work is downloaded from Delft University of Technology.
For technical reasons the number of authors shown on this cover page is limited to a maximum of 10.

Green Open Access added to TU Delft Institutional Repository

'You share, we take care!' - Taverne project

https://www.openaccess.nl/en/you-share-we-take-care

Otherwise as indicated in the copyright section: the publisher is the copyright holder of this work and the author uses the Dutch legislation to make this work public.

Journal of Hydrology 617 (2023) 129088

Contents lists available at ScienceDirect

Journal of Hydrology

journal homepage: www.elsevier.com/locate/jhydrol

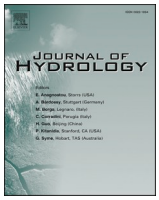

Research papers

Crevasse splay morphodynamics near a non-vegetated, ephemeral river terminus: Insights from process-based modelling

Jiaguang Li [a,b,*], Helena van der Vegt [c], Joep E.A. Storms [d], Stephen Tooth [e]

[a] Key Laboratory of Tectonics and Petroleum Resources (China University of Geosciences), Ministry of Education, Wuhan 430074, China
[b] Key Laboratory of Theory and Technology of Petroleum Exploration and Development in Hubei Province, Wuhan 430074, China
[c] Deltares, Boussinesqweg 1, 2629 HV Delft, The Netherlands
[d] Faculty of Civil Engineering and Geosciences, Delft University of Technology, P.O. Box 5048, 2628CN Delft, The Netherlands
[e] Department of Geography and Earth Sciences, Aberystwyth University, Aberystwyth SY23 3DB, UK

ARTICLE INFO

This manuscript was handled by Emmanouil Anagnostou, Editor-in-Chief, with the assistance of Giulia Sofia, Associate Editor

Keywords:
Backflow
Channel-floodplain morphodynamics
Crevasse splay
Discharge
Dryland river

ABSTRACT

Crevasse splays generate subtle local relief and contribute to fluvial basin sedimentary filling but controls on splay development along dryland rivers remain poorly understood owing to limited field, laboratory, and numerical modelling studies. Based on previously-acquired field data and new remote sensing observations of splay morphology and sedimentology (e.g. slope, width, length, grain size) and flooding characteristics (e.g. discharge, water depth and extent) near the terminus of the non-vegetated, ephemeral Río Colorado on the southeastern margin of Salar de Uyuni, Bolivia, we undertake process-based modelling using Delft3D to isolate the role of hydrological controls on crevasse splay morphodynamics. Holding the potential sediment supply constant, we focus on the role of discharge (outflow from trunk channel to crevasse channel during rising stage), floodplain water levels, and backflow (reflux to the trunk channel during falling stage). Using nine different model runs, each with 10 simulated flood cycles, we show that the processes associated with these hydrological controls result in various outcomes, from short crevasse splay channels that may bifurcate and develop depositional bars to longer splays with one primary channel that mainly transfers sediment across the floodplain. Results reveal that increases in flood discharge lead to more rapid splay sedimentation and stabilization of a single crevasse channel. Increases in floodplain water level lead to shorter but wider splays and facilitate the formation of multiple stable crevasse channels. High floodplain water levels probably restrict splay length owing to deceleration of outflow as floodplain water is encountered, but separate crevasse channels may form downstream as backflow breaches the trunk channel levee during falling stage. These findings support and extend previous observations from the Río Colorado and other dryland rivers worldwide. Future modelling studies that consider a wider range of hydrological, sedimentological, and floodplain topographic conditions will help develop more comprehensive numerical models of splay development. A combination of insights from field, laboratory experimentation, remote sensing and modelling will improve knowledge of the cascades of channel-floodplain dynamics that characterise many dryland endorheic basins.

1. Introduction

Along river systems, floods that start to exceed bankfull spread beyond the confines of the channel, leading to overbank flow and the initiation of various channel-floodplain interactions. Rapidly changing flood hydraulic conditions are associated with shifting erosional and depositional patterns, thereby influencing local topographic relief, and down-valley and cross-valley water and sediment transfer (e.g. Mertes et al., 1996; Walling and He, 1998; Pizzuto et al., 2008; Lewin et al., 2017). Along some rivers, overbank flow can trigger levee breaching and initiate crevasse channel formation on proximal floodplain areas (Miall, 1996; Bridge, 2003). Once formed, crevasse channels can increase flow and sediment diversion from the trunk channel (sometimes termed the main or parent channel), commonly leading to splay erosion and deposition on more medial and distal floodplain areas. Over time, continued development and local coalescence of splays can help build alluvial ridges, and may also prime river reaches for avulsion (Smith and Perez-Arlucea, 1994; Bristow et al., 1999; Tooth, 2005; Buehler et al.,

* Corresponding author at: Key Laboratory of Tectonics and Petroleum Resources (China University of Geosciences), Ministry of Education, Wuhan 430074, China.
E-mail addresses: jiaguangli@cug.edu.cn, jiaguangli@gmail.com (J. Li).

https://doi.org/10.1016/j.jhydrol.2023.129088
Received 4 January 2022; Received in revised form 29 November 2022; Accepted 5 January 2023
Available online 7 January 2023
0022-1694/© 2023 Elsevier B.V. All rights reserved.

2011; Li et al., 2014), ultimately leading to more widespread lateral redistribution of water and sediment. Over longer timescales, therefore, splays and avulsions can be a key influence on the filling and sedimentary architecture of fluvial basins (Miall, 1996; Bridge, 2003; Slingerland and Smith, 2004).

Using field, laboratory, and conceptual and numerical modelling approaches, crevasse splays and their association with channel-floodplain processes such as avulsion have been widely studied, particularly along present-day humid-region, perennial river systems (e.g. Slingerland and Smith, 1998; Stouthamer, 2001; Aslan et al., 2005; Hajek and Wolinsky, 2012; Kleinhans et al., 2013; Hajek and Edmonds, 2014; Shen et al., 2015; Millard et al., 2017; Nienhuis et al., 2018; Rahman et al., 2022). This body of research has enabled many key controls on splay development to be identified, including those relating to discharge, water surface and land surface gradients, floodplain vegetation and drainage conditions, and sediment supply, cohesion and consolidation. Over the last few decades, improved understanding of the interactions among these controls has provided the basis for the use of splays as a deliberate management tool; for instance, creating artificial diversions that mimic splays and thereby help to control basinward water and sediment fluxes (e.g. Florsheim and Mount, 2002; Yuill et al., 2016; Nienhuis et al., 2018).

By contrast with the research on humid-region river systems, far less is known about crevasse splays along present-day dryland river systems. Some of the aforementioned studies have generated insights about splay development that may be applicable to dryland systems. For instance, the broad controls, preconditioning factors, and formative processes of splay development (e.g. levee breaching, crevasse channel formation and flow and sediment diversion) may be similar between humid-region and dryland rivers (Tooth, 2005; Li et al., 2014; Li and Bristow, 2015; Rahman et al., 2022). Nonetheless, it remains unclear the extent to which different flooding characteristics along many dryland rivers – particularly the typically more rapid rise and fall of flood stage, and the long periods of little or no flow along ephemeral or intermittent rivers – influence the spatial patterns, rates and timescales of splay development (Reid and Frostick, 2011; Tooth and Nanson, 2011; Tooth, 2013). Rare descriptions of dryland river splays have formed part of broader investigations of the channel-floodplain morphodynamics along the lower reaches of moderately vegetated, relatively coarse-grained (sand, minor gravel), ephemeral rivers in endorheic basins, such as characterise the 'floodout zones' (e.g. Tooth, 1999a,b, 2000, 2005; Millard et al., 2017; Li et al., 2019) and 'terminal splay' complexes in central Australia (e.g. Lang et al., 2004; Fisher et al., 2008). In recent years, research has also been directed towards channel-floodplain morphodynamics in the lower reaches of sparsely or non-vegetated, typically finer grained (mud, fine sand), ephemeral rivers (e.g. Donselaar et al., 2013; Ielpi, 2018; Ielpi and Lapôtre, 2019a,b; Li et al., 2019, 2020a,b, 2022). In large part, this new research focus has been due to the potential use of such rivers as modern analogs for unconventional hydrocarbon reservoirs and pre-Silurian rock records (Li et al., 2014, 2015, 2020b; Ielpi, 2018; Ielpi and Lapôtre, 2019a; van Toorenenburg et al., 2016, 2018; Donselaar et al., 2022).

A prime example of a non-vegetated, fine-grained, ephemeral river with abundant splays is the lower Río Colorado, Bolivia (Fig. 1). The lower part of the river system is an example of a distributive fluvial system (DFS, *sensu* Weissmann et al., 2010), and consists of the active (trunk) channel, numerous partially active and abandoned channels, and a topographically complex floodplain (Li et al., 2019). Channel planforms range from straight to sinuous, partly depending on the time elapsed since initial formation, with channels tending to become more sinuous over time (Li et al., 2019; Donselaar et al., 2022). The trunk channel terminates on the southeastern margin of Salar de Uyuni, the world's largest salt lake (Fig. 1A-C). The absence of vegetation along the channels and on the floodplain is due to the characteristically dry and saline environment (Fig. 1C-F). Previous studies have provided valuable insights into the processes, patterns and rates of splay development

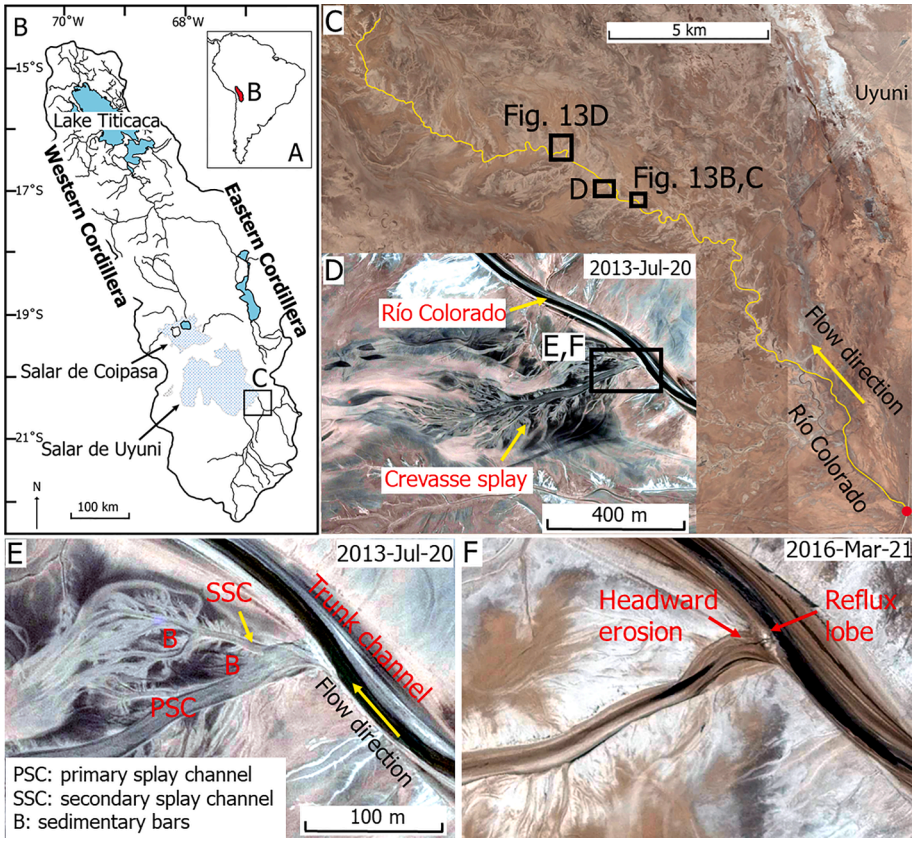

Fig. 1. Characteristics of the Altiplano and the lower Río Colorado: (A) location of the Altiplano in South America; (B) map of the Altiplano showing the location of the study reach (modified after Placzek et al., 2013); (C) the lower reaches of the Río Colorado approaching the southeastern margin of Salar de Uyuni, with the black boxes indicating the locations of the satellite imagery used in part D and Fig. 13B-C and Fig. 13D; (D) high-resolution satellite image of a typical crevasse splay, with the black box indicating the locations of parts E and F; (E) and (F) details of the junction between the trunk channel and the crevasse channel illustrated in part D for two different dates, illustrating key elements of crevasse splay development, including the initial multiple splay channel network, later stage headward erosion of the primary splay channel, and formation of a reflux lobe by backflow.

(Donselaar et al., 2013, 2022; Li and Bristow, 2015; van Toorenenburg et al., 2018), but many uncertainties remain, especially regarding the relative importance of hydrological variations such as discharge, rates of stage rise and fall, and overbank flooding depth and extent. The river is ungauged, and during floods the study area is largely inaccessible so direct flow and sediment transport measurements cannot be made. Nonetheless, hydraulic reconstructions using a combination of field measurements, remote sensing image analysis, and numerical modelling can still generate key data on channel and overbank flood characteristics (e.g. Li et al., 2018, 2020c).

Further valuable insights into the controls on splay morphodynamics along the lower Río Colorado can be provided by a process-based modelling approach. In this paper, we outline the study area and summarise previous work on the splays of the lower Río Colorado in order to isolate the key hydrological controls. Thereafter, our aims are to: 1) use Delft3D to investigate the relative importance of these hydrological controls (specifically discharge, floodplain drainage conditions, and backflow) in the initiation and development of crevasse splays along the Río Colorado; 2) compare the controls, patterns, processes and rates of splay development along the Río Colorado with splay formation along other dryland rivers; 3) evaluate the modelling results in relation to those derived from other splay modelling studies; and 4) consider how numerical modelling approaches can be developed to provide further insight into crevasse splay and associated channel-floodplain morphodynamics along dryland rivers more generally.

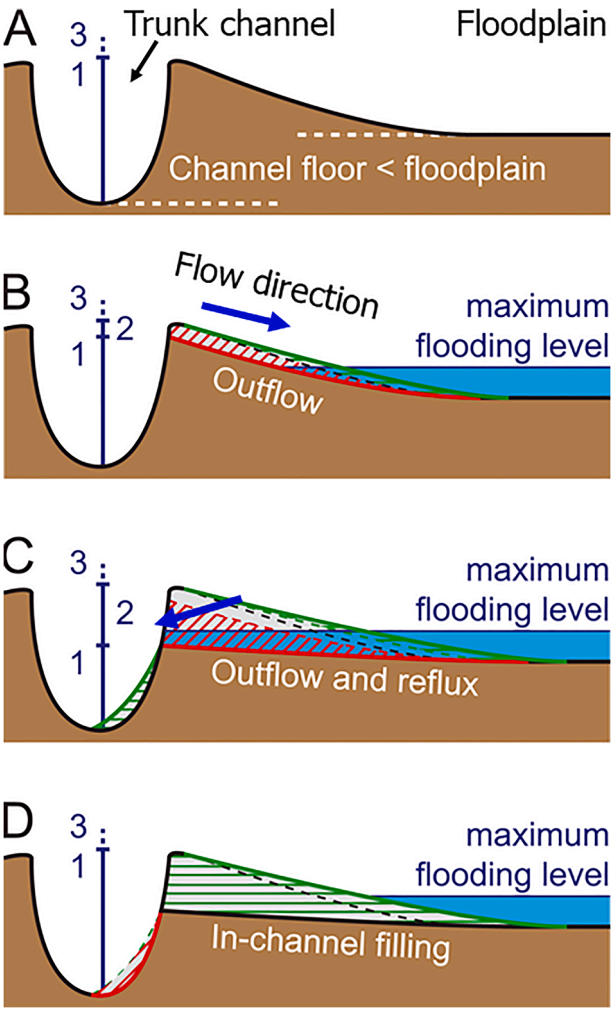

Fig. 2. Conceptual diagram (not to scale) of the generic life cycle of a crevasse splay where the maximum flooding level on the floodplain remains lower than the levee elevation (from van Toorenenburg et al., 2018). Trunk channel water level varies over time and corresponds with confined in-channel flow (1), crevasse-confined flooding (2), and unconfined overbank flooding (3). In parts B through D, the initial floodplain topography (part A) is indicated by a sloping, black dashed line. Erosion of the crevasse and splay channel bed is indicated in red (parts B-C). Adjacent deposition on levees, in splay lobes, and the trunk channel bed (reflux lobe) is indicated in green (parts B-C). Ultimately, the crevasse and splay channel infills, and the reflux lobe is eroded (part D). (For interpretation of the references to colour in this figure legend, the reader is referred to the web version of this article.)

2. Study area and previous work on the splays of the lower Río Colorado

Over the last decade, a combination of field data, high-resolution satellite imagery, and conceptual and numerical modelling has been used to document the flood hydrology and channel-floodplain morphodynamics approaching the terminus of the Río Colorado, and assess the sedimentological implications (e.g. Donselaar et al., 2013, 2022; Li et al., 2014, 2018, 2019, 2020a,b; Sandén, 2016; van Toorenenburg et al., 2018). Similar to the lower reaches of many other ephemeral dryland rivers, there is a significant downstream decrease in the cross-sectional area of the river from ~80 m^2 to <5 m^2 and its associated sediment transport capacity (Donselaar et al., 2013, 2022). These changes lead to widespread overbank flow during floods, which typically occur approximately once annually, but with flood clusters being closely related to La Niña-like conditions (Li, 2014; Li et al., 2020a,c, 2021). Approaching the river terminus, bed, bank and floodplain sediment is dominantly fine-grained (D_{50} < 60 μm) but there are no data on bedload or suspended sediment loads during floods owing to the absence of gauges and lack of real-time monitoring and measurement (Li et al., 2015). Overbank flow commonly initiates levee breaching along the trunk channel and other partially active channels, resulting in a downstream increase in the number of crevasse splays (Li and Bristow, 2015). Formation of multiple crevasse splays with local relief up to ~0.5 m (Fig. 1D-F) commonly leads to lateral amalgamation and vertical stacking, resulting in low accommodation space on the floodplain adjacent to the channels (Li et al., 2014; Li and Bristow, 2015). Consequently, during waning flood stages, significant volumes of overbank floodwater can flow back towards the channels through some of the crevasse splay networks, a process termed backflow or reflux (e.g. van Toorenenburg et al., 2018). Due to limited accessibility during peak floods, field measurements of flood flow conditions are notoriously difficult and real-time observations using remote sensing approaches are commonly limited by satellite visiting periods, resolution, and/or cloud cover (e.g. Li et al., 2018). Nevertheless, based on pre- and post-flood field observations of the lower Río Colorado, van Toorenenburg et al. (2018) distinguished three different splay types, namely: i) splays subject to unidirectional (basinward) drainage; ii) splays facilitating bidirectional drainage; and iii) splays in a post-active abandonment phase. From these observations, van Toorenenburg et al. (2018) proposed a generic life cycle for crevasse splays that spans multiple flooding events (Fig. 2). Initial splay development is controlled dominantly by outflow from the trunk channel, which initiates crevasse channel erosion and associated deposition as the splay channels adjust towards an equilibrium profile graded to a local base level formed by their distal termini. At this stage, the bed elevation at the crevasse channel apex remains higher than the maximum flood (ponding) depth on the floodplain and there is no backflow (reflux) to the trunk channel (Fig. 2). Continued incision during subsequent floods along the crevasse channel, however, lowers the bed elevation at the crevasse apex to below the maximum flood depth on the floodplain. Coupled with more distal deposition, these morphodynamic adjustments facilitate the return flow of water and sediment to the trunk channel during falling stage (Fig. 2). Temporarily, this lowers or reverses the equilibrium profile, with local base level now formed by the lower elevation trunk channel thalweg. As

a consequence, headward erosion (the 'backstepping erosion' of van Toorenenburg et al., 2018) commonly occurs throughout the splay channel network, and the increased sediment supply can promote the formation of reflux lobes at the junction with the trunk channel (cf. Fig. 1F). This lowering or reversal of crevasse channel gradient ultimately leads to lower velocity outflows from the trunk channel during floods, which may then lead to backfilling and abandonment of the crevasse splay (Fig. 2).

The field observations of van Toorenenburg et al. (2018) draw particular attention to the key controls on splay development in this setting, including: i) the relative channel and floodplain gradients; ii) the relative elevations of the trunk channel bed, crevasse channel bed and floodplain; and iii) the relative floodwater depths in the trunk channel and on the floodplain. While their conceptual model provides numerous useful insights into splay development, the dynamic interplay between these factors under various flooding scenarios remains to be explored more comprehensively using numerical modelling approaches. Significantly, however, van Toorenenburg et al.'s (2018) observations highlight the limitations of previously published modelling experiments for investigating the relative role of these controls in splay development in the Río Colorado setting. Two contrasting examples illustrate this point. Slingerland and Smith's (1998) physically-based conceptual model of the development of an initial crevasse channel highlighted the importance of the amount of suspended sediment delivered to the crevasse channel relative to its transport capacity but did not consider the conditions leading to the initial crevasse formation, or the role of bedload, variations in outflow, or backflow. Millard et al.'s (2017) numerical model aimed to isolate how sediment supply and floodplain drainage conditions influence splay growth but their model setup represented a flat-floodplain condition that was designed explicitly to promote deposition and limit channelisation and sediment remobilisation that may arise from flow over a sloped floodplain. In their model, an initial crevasse and associated levees had a non-erodible base and morphodynamically developed only through deposition. While providing many useful insights, therefore, the limitations of these and other numerical models restrict direct application of the previously published modelling results to the Río Colorado setting.

In short, the controls of crevasse splay development along the Río Colorado — and potentially along other similarly low-gradient, non-vegetated, dryland rivers (e.g. Ielpi, 2018; Ielpi and Lapôtre, 2019a,b) — are still not fully understood. Using Delft3D, a process-based numerical model, in this paper we test and extend van Toorenenburg et al.'s (2018) field-based observations by addressing the role of hydrological variations in crevasse splay formation. Specifically, this study focuses on the relative importance of discharge (outflow from trunk channel to crevasse channel during rising stage) and backflow (reflux to the trunk channel during falling stage) in the early stages of crevasse splay formation. The early stages of crevasse splay development have been reported to have a fundamental impact on later splay growth and therefore the subsequent architecture of splay deposits (Toonen et al., 2016). Similar to other splay modelling studies where simplifying assumptions have been made (e.g. Slingerland and Smith, 1998; Millard et al., 2017; Nienhuis et al., 2018), in order to isolate and evaluate the relative influence of these hydrological controls, at this stage we do not address sediment supply variations.

3. Methods and model setup

3.1. Numerical model

We used the open-source physics-based model, Delft3D (version 4.04.01), to conduct numerical experiments linking hydrodynamic, sediment transport and morphological changes in the early stages of crevasse splay development. Delft3D solves the two-dimensional depth-averaged flow equations and computes sediment transport and bed level change (Lesser et al., 2004). The reliability and accuracy of this model for both scientific research and engineering practice has been demonstrated in a wide spectrum of river, estuarine and coastal systems (e.g. Mosselman, 2004; Edmonds and Slingerland, 2007, 2008; Schuurman et al., 2013; Hajek and Edmonds, 2014; Yuill et al., 2016; Millard et al., 2017; Nienhuis et al., 2018; David et al., 2018). Compared with other numerical models, a particular advantage of Delft3D is its simulation of sediment transport and morphodynamics with rigorous theoretical foundation (Mosselman, 2004; Edmonds and Slingerland, 2007, 2008; Schuurman et al., 2013).

The hydrodynamics in Delft3D are based on conservation of momentum and mass assuming hydrostatic pressure. The equations of fluid motion, sediment transport and deposition are discretized on a 3D curvilinear, finite-difference grid, and an alternating direction implicit scheme is used to solve the differential equations (for detailed descriptions of the hydrodynamics and numerical scheme of Delft3D, see Lesser et al., 2004).

3.2. Model setup and input

This study focuses on channel-floodplain interactions during overbank flooding, particularly during and after peak discharge. Accordingly, we created a schematized model to investigate morphodynamics of a trunk channel and an adjacent right-hand floodplain. Based on width and depth measurements of the Río Colorado approaching the river terminus (Donselaar et al., 2013), the trunk channel was set at 300 m long, 32 m wide and 2 m deep (Fig. 3). Measurements of 216 crevasse splays approaching the Río Colorado River terminus (Li and Bristow, 2015) reveal that the median values of splay length and width are 298 m and 112 m, respectively. Based on these dimensions, the levee and floodplain in the model domain was set at 300 m long × 368 m wide (Fig. 3). A 40 m wide levee, initially without crevasse channels, was set uniformly along the edge of the trunk channel with a cross-valley slope of 0.5 %, while the rest of the domain was floodplain with a cross-valley slope of 0.09 % (Fig. 3). A high resolution (2 m × 2 m) grid cell for observation of channel-floodplain morphodynamics was set uniformly across the model domain.

Differential GPS field measurements reveal that cross-valley gradient prominently exceeds downvalley (basinward) gradient (i.e. along and parallel to the trunk channel) in this low-gradient system (Li et al., 2015a, 2019, 2020c; van Toorenenburg et al., 2018). Owing to the low downvalley gradient (Table 1) and the short length (300 m) of the modelled reach, the downvalley elevation fall in the model domain is negligible, and the model runs are dependent mainly on the levee, floodplain cross-valley, and water surface gradients. The model runs employ a straight channel with an initially flat channel bed to avoid topographic forcing and allow crevasse splays to form entirely as the result of the physical and constitutive relations (Schuurman et al., 2013). On the modelling timescale, flooding is driven by variations in river discharge. Initially, water flows down the trunk channel. Then, as stage rises, erosion and outflow occurs through newly forming crevasse channels, leading to floodplain inundation. Finally, as stage falls, reflux returns flow to the main channel. Accordingly, we set two open boundaries for the trunk channel with upstream inflow and downstream outflow, as well as open boundaries at either edge of the floodplain domain (Table 1, Fig. 3). The trunk channel inflow boundary is characterized by a constant frequency of peak flow and low flow (i.e. a fixed flood return period). As such, water level at the outflow boundary is set for two conditions: a low flow water level (6 m) during the low discharge period and a peak flow water level (6.5 m) for the peak discharge, where the water levels are relative to the top elevation of the maximum initial sediment thickness in the model domain. In the model domain (Fig. 3), this peak flow water level equates to a channel water depth of 2 m and an overbank water depth of up to 0.5 m.

Time series of high-resolution satellite imagery has revealed that crevasse splays along the Río Colorado tend to develop in the austral summer when most rainfall and flooding occurs. More than three

decades of daily precipitation data (1985–2017) reveal that peak flooding occurs approximately once per year on average, although there may be clusters of floods as driven by ENSO cycles (Li and Bristow, 2015; Li et al., 2019, 2020a, 2021). To fully capture the rise and fall of typical hydrographs in the river system, a morphological factor (morFac) of 10 was set, and ten flood cycles, each with a simulation time of 52 h, were employed. The morphological factor reduces computational time by accelerating the morphological response to each hydrodynamic timestep by the value set (Lesser et al., 2004).

Sediment input in the model was based on the analysis of the grain-size distribution of 219 samples collected from the lower reaches of the Río Colorado. Samples were collected mainly from point bar deposits, and crevasse splay and floodplain sediments, and are mostly composed of fine sand, silt and clay (Li et al., 2015). Based on the field data, in the model we set a ratio of 2:3:3 for fine sand, silt and clay (Table 2). The Engelund-Hansen equation (Engelund and Hansen, 1967) was used to calculate sediment transport for non-cohesive sediment. As one of our study aims was to investigate the relative importance of hydrological controls in crevasse splay initiation and development, for the upstream boundary, a constant potential sediment supply was assigned to all simulations. Therefore, model runs with a larger discharge were supplied with more sediment overall than model runs with smaller discharges (Morehead et al., 2003).

We simulated nine different model runs, each of which has ten cycles of peak discharge and backflow (Table 3, Fig. 4). The model runs were designed to highlight the relative importance of hydrological controls on key erosional and depositional processes: specifically, discharge, and the combined effect of floodplain water level and backflow. To help differentiate the impact of overbank flow and backflow, three phases were defined for each flood cycle (Fig. 4): phase 1 is from the start of a new flood to the flood peak; phase 2 is from the end of peak flow to the start of backflow; and phase 3 is before the new flood cycle starts. The 'discharge model' runs (M1 to M5) have a fixed floodplain water level of 6.5 m but different discharges of 50, 60, 70, 80 and 90 m^3/s, respectively (Fig. 4A). The 'backflow model' runs (M6, M7, M2, M8, M9) have a fixed discharge of 60 m^3/s but different floodplain water levels of 6.3, 6.4, 6.5, 6.6 and 6.63 m, respectively. With its common discharge of 60 m^3/s and floodplain water level of 6.5 m, model run M2 is included in both the discharge and backflow model runs, and so provides a reference model for comparison across the full suite of model runs. With reference to the non-crevassed levee elevation of 6.5 m, model runs M6 (6.3 m) and M7 (6.4 m) have water levels lower than the levee, model run M2 has a water level equal to the levee elevation, and model runs M8 (6.6 m) and M9 (6.63 m) have water levels higher than the levee (Fig. 4B).

For each model run, a transition from no water to low (confined) flow of 10 m^3/s was set initially to ensure model stability. Each flood cycle then starts from this low flow discharge (Fig. 4) and subsequently linearly increases to peak discharge. Bankfull discharge (~50–60 m^3/s) was estimated using Bjerklie's (2007) model, which has been successfully applied for discharge estimation along the Río Colorado and other ungauged dryland rivers (Larkin et al., 2017; Li et al., 2019, 2021). As discharge increases, overbank flow initiates from upstream to downstream, and water level increases on the floodplain. As peak discharge is passed, and stage in the trunk channel begins to fall, backflow from the floodplain to the trunk channel potentially can start. The termination of backflow events is followed by evaporation (modelled using heat flux equations, for details, see page 227 in the Delft3D-FLOW User Manual), which removes water on the floodplain prior to the next flood (Fig. 4). Based on previous work in this study area (Li et al., 2020c), a Manning roughness coefficient of 0.03 is used in the model.

Table 1
Initial conditions and default input parameters for the Delft3D model used in this study, as based on the characteristics of the lower Río Colorado channel and floodplain. The lower Río Colorado is low gradient (0.05 % or 0.0005 m m^{-1}); hence, for this short (300 m long) modelled reach, bed slope is set to zero, with flow driven by time-series discharge in the upstream boundary and various water levels at the downstream boundaries.

Parameter	Unit	Value
Main channel length	m	300
Main channel width	m	30
Bed slope	m/m	0
Floodplain slope		0.09 %
Levee slope		0.50 %
Grid cell length	m	2
Grid cell width	m	2
Hydrodynamic time step	s	0.0025 min (0.15 s)
Sediment transport predictor	kg m^{-1} s^{-1}	Engelund-Hansen
Peak discharge	m^3/s	60
Low discharge	m^3/s	10

3.3. Post processing

Channel-floodplain morphodynamics, sediment thickness, and flow velocity and bed shear stress for each flood cycle were analyzed. The sedimentary features near open boundaries (e.g. upstream bars near the inflow boundary) were not subjected to further analysis to avoid including unrealistic boundary effects. Three downvalley floodplain profiles were analyzed, with the profiles taken parallel to and away from the trunk channel at distances of 200 m, 250 m and 300 m. Key morphological elements, including crevasse channels and depositional

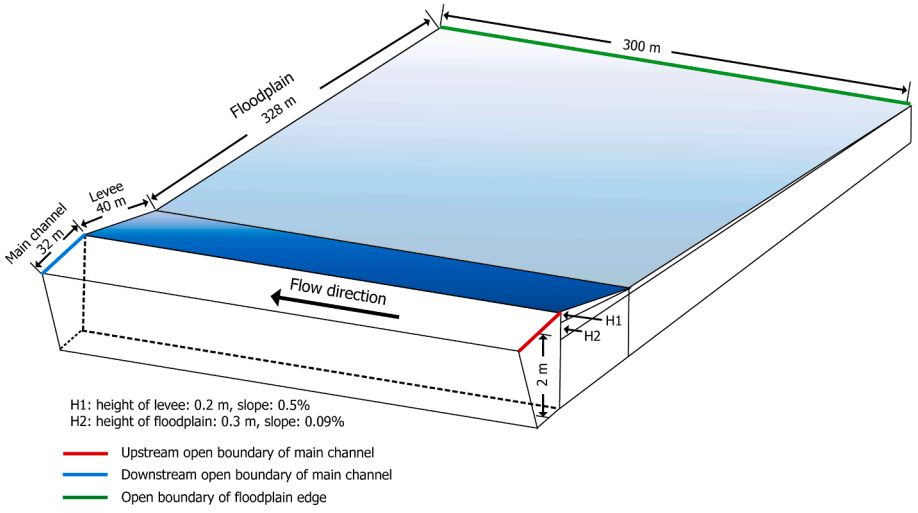

Fig. 3. Schematic diagram of the model domain and boundaries used in this study.

bars, were identified along these profiles and their morphodynamics were recorded on the basis of topographic changes. For crevasse channels, the lowest topographic points on each profile were extracted (i.e. bed level), while for bars, the highest topographic points on each profile were extracted (i.e. bar tops). High-resolution satellite imagery (dates 2010, 2013, 2016, 2018) from Google Earth Pro reveal crevasse splay morphodynamics along the Río Colorado over the last decade (e.g. Fig. 1D-F), and were compared with the model outputs using visual inspection.

4. Results

Based on the hydrological, sedimentological and geomorphological characteristics of the lower Río Colorado, our Delft3D generic simulations systematically varied the flood discharge and floodplain water levels. As outlined below, our results show that increases in discharge lead to more rapid splay sedimentation and stabilization of a single crevasse channel. Increases in floodplain water level result in short, wider splays and facilitate the development of multiple stable crevasse channels.

4.1. Reference model run (M2)

The reference model run illustrates that ten flood cycles are sufficient to fully capture the early stage of crevasse splay development that result from overbank flooding and backflow processes (Fig. 5). The crevasse splay complex ultimately includes two crevasse channels, namely a primary splay channel (PSC) and a secondary splay channel (SSC), and three depositional bars (downstream bar, middle bar and distal bar) (Fig. 5H).

At the start of the model run (1st flood), overbank flooding occurs in the upstream reach of the trunk channel, and is associated with pronounced levee breaching (Fig. 5A). Adjacent to the breached levee, two splay channels develop on the floodplain, both of which lengthen, narrow and deepen by erosion during the first few floods (Fig. 5A-D; Fig. 6). The splay channel that is located perpendicular to the trunk channel develops more rapidly and eventually becomes the PSC (Fig. 5E-F). From the 7th flood onwards, this channel stabilizes in width (Fig. 5G-J; Fig. 6). A SSC develops during the first three flood cycles (Fig. 5A-C; Fig. 6) but subsequently shallows and narrows as the middle bar and downstream bar grow in size, albeit at a slower rate after the 6th flood (Fig. 5D-J; Fig. 6). In later flood cycles, a distal bar develops (e.g. Fig. 5G-I) and eventually amalgamates with the middle bar (Fig. 5J).

Analysis of the simulated topography shows that the PSC experiences erosion, albeit with a decrease in depth from the proximal (1.25 m difference) to distal (1.03 m difference) region (Fig. 6; Fig. 7A-C, M2, red line with circles). In the proximal profile (200 m), for each flood cycle, the PSC bed experiences minor deposition around the flood peak but erosion exceeds this deposition during backflow phases, leading to an overall erosive trend (Fig. 6A; Fig. 7A: M2, red line with circles). The elevation change over time in the proximal section (200 m) is "staggered" with relatively pronounced depositional and erosional events during the different phases of the flooding cycle (Fig. 7A) while the medial profile (250 m) and the distal profile (300 m) show a "smoother" decrease in elevation over time (Fig. 7B-C).

The SSC is characterized by a fluctuating trend from overall deepening (erosion) to shallowing (filling) through the 10 flood cycles (Fig. 6; Fig. 7D-F: M2, red line with circles). During the 1st to the 6th flood cycles, the net elevation of the SSC decreases in the proximal profile, with pronounced erosion during backflow phases overriding any deposition occurring in the other phases of the flooding cycles (Fig. 6; Fig. 7D). From the 7th flood cycle onwards, the elevation of the SSC shows a slight net increase, with the erosion in the backflow phase no longer overriding the deposition experienced in the other phases (Fig. 6; Fig. 7D). The medial (250 m) and distal (300 m) profiles show similar trends, with initial minor erosion followed by minor filling (Fig. 6; Fig. 7E-F).

The middle bar undergoes minor variations in elevation away from the trunk channel. The proximal (200 m) profile shows that erosion occurs in the backflow phase of the 1st flood cycle but thereafter deposition predominates until the bar elevation stabilises from the 7th flood cycle onwards (Fig. 6; Fig. 7G: red line with circles). In the medial (250 m) and distal (300 m) profiles, the middle bar experiences an increase in elevation during the first 4 or 5 flood cycles and thereafter stabilises (Fig. 6; Fig. 7H-I).

4.2. Discharge model runs (M1 to M5)

In comparison to M2, the other four discharge model runs have discharges that are either smaller (M1) or larger (M3 to M5). The results show that differences in peak discharge have a strong influence on the crevasse splay morphodynamics (Fig. 7; Fig. 8). In simulations with smaller and larger peak discharges, only a PSC fully develops and there is either no evidence or only weak development of a SSC and middle bar (Fig. 7; Fig. 8).

For the lowest discharge model (M1), levee breaching occurs but this only leads to limited development of a PSC (Fig. 8). During the backflow stage, all water drains back to the trunk channel via the PSC. Elevation analysis shows that in model run M1, the PSC in the proximal (200 m) profile is deeper than in model run M2 for the first eight floods (Fig. 7A: blue line with crosses) but in the more medial (250 m) and distal (300 m) profiles is noticeably shallower (Fig. 7B-C). For simulations with larger peak discharge (M3 to M5), levee breaching tends to occur slightly farther downstream along the trunk channel, and a PSC becomes increasingly prominent, leading to increasing sediment transfer to and across the full width of the floodplain (Fig. 8). In M3, M4 and M5, the bed level of the PSC decreases initially but approaches a stable elevation

Table 2
Parameters of sediment composition used in the Delft3D model in this study.

Composition 1: Fine sand	
Median value (D_{50}, μm)	100
Dry bed density (kg m^{-3})	1600
Composition 2: Silt	
Dry bed density (kg m^{-3})	500
Settling velocity (m/s)	1
Critical bed shear stress for sedimentation (N/m^{-2})	1000
Critical bed shear stress for erosion (N/m^{-2})	0.5
Erosion parameter (kg m^{-2} s^{-1})	0.0001
Composition 3: Clay	
Dry bed density (kg m^{-3})	500
Settling velocity (m/s)	0.5
Critical bed shear stress for sedimentation (N/m^{-2})	1000
Critical bed shear stress for erosion (N/m^{-2})	0.8
Erosion parameter (kg m^{-2} s^{-1})	0.0001

Table 3
Delft3D model setups in this study. Note that M2 is a reference model and is included in both the discharge and backflow models. In the model domain (see Fig. 3), a floodplain water level of 6.5 m corresponds to a channel water depth of up to 2 m and an overbank water depth of up to 0.5 m (see text for further explanation).

Model number		Discharge (m^3/s)	Floodplain water level (m)
Discharge models	M1	50	6.5
	M2	60	6.5
	M3	70	6.5
	M4	80	6.5
	M5	90	6.5
Backflow models	M6	60	6.3
	M7	60	6.4
	M2	60	6.5
	M8	60	6.6
	M9	60	6.63

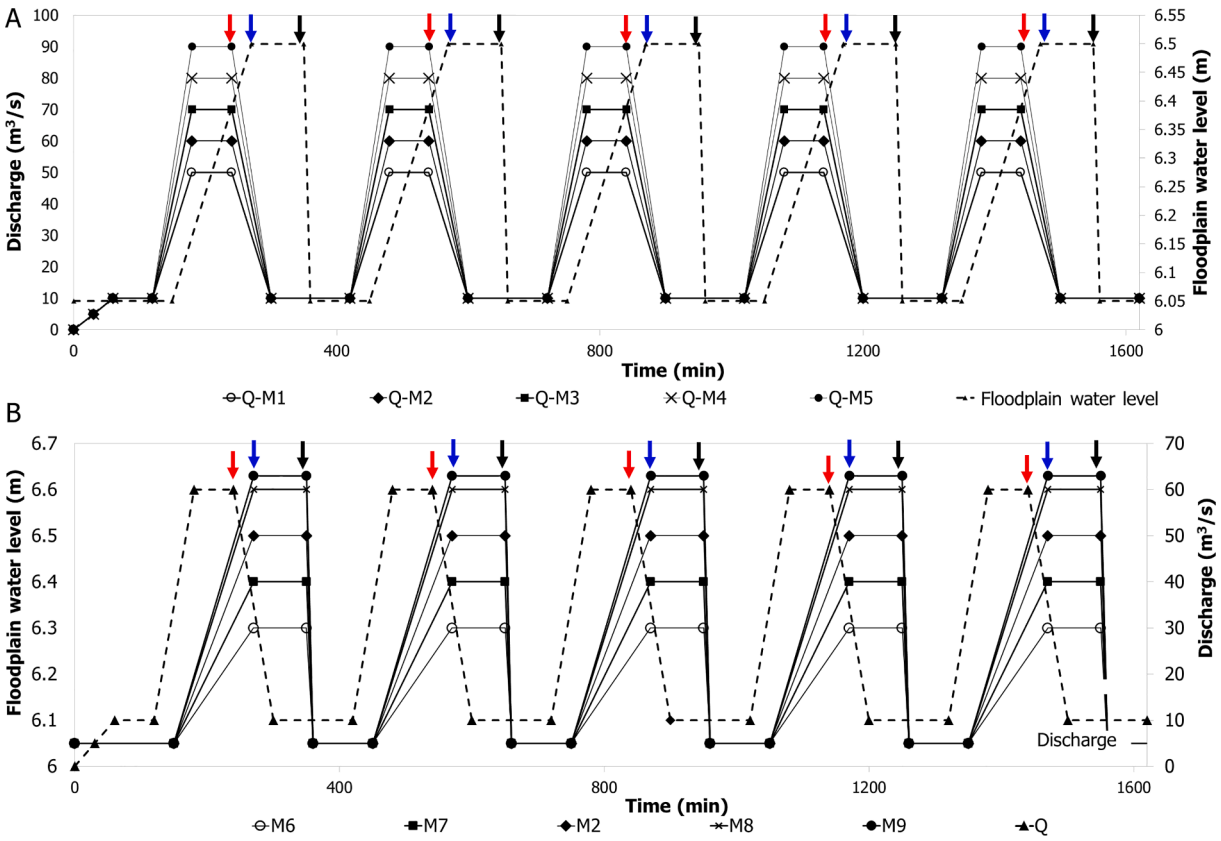

Fig. 4. Discharge and floodplain water levels for the different model runs (only the first five of the ten flood cycles are shown, with the remaining five cycles being the same as the first five): (A) discharge model runs (M1-M5) with varying discharges but fixed floodplain water level; (B) backflow model runs (M6, M7, M2, M8, M9) with varying floodplain water levels but fixed discharge. M2 is a reference model that is included in both A and B and floodplain water level is with reference to the bottom elevation of the model. Arrows with different colors indicate the end of various phases of single flood cycles: phase 1 (red); phase 2 (blue); and phase 3 (black). (For interpretation of the references to colour in this figure legend, the reader is referred to the web version of this article.)

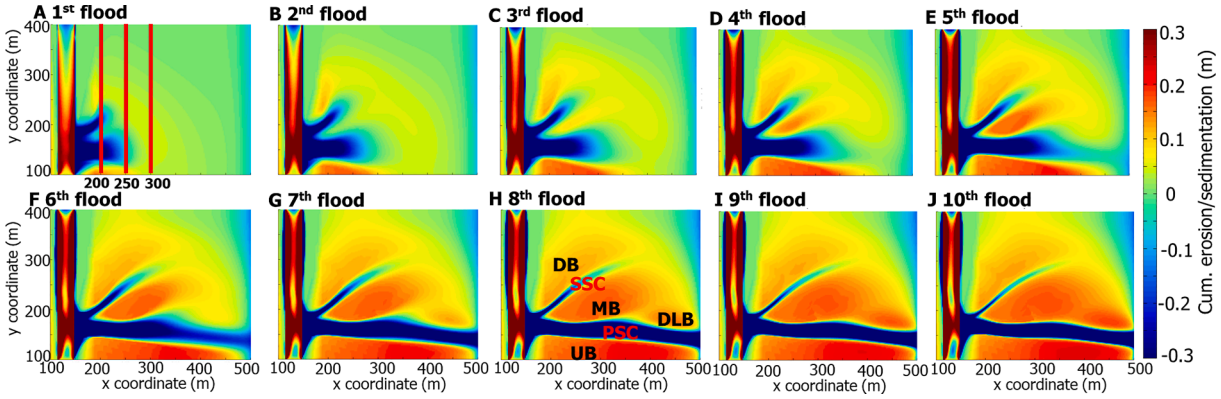

Fig. 5. Patterns of cumulative erosion and sedimentation during the 10 flood cycles for the reference model (M2). The location of the floodplain topographic profiles at 200 m, 250 m and 300 m from the trunk channel (Figs. 6, 7 and 9) are shown in A (1st flood cycle). Key morphosedimentary features are labelled on H (8th flood cycle): PSC: primary splay channel; SSC: secondary splay channel; UB: upstream bar; MB: middle bar; DB: downstream bar; DLB: distal bar. Note that the upstream bar (UB) is not analyzed owing to potential boundary effects.

in the later flood cycles, especially in the more proximal reaches (Fig. 7A-C).

In simulations with discharges larger (M3-M5) than the reference model (M2), a SSC develops in the initial flood cycles but then disappears (Fig. 7D-F; Fig. 8). Owing to the limited development of a SSC in models runs M1 and M3 to M5, a middle bar remains poorly defined. In M3 and M4, deposition initially results in a vertically accreting middle bar and then greater stability after the 3rd flood cycle in the proximal and medial parts, and greater stability after the 7th flood cycle in the more distal parts (Fig. 7G-I). The SSC is eliminated when the middle bar accretes laterally to fill the SSC (e.g. Fig. 8C and 8H).

4.3. Backflow model runs (M2, M6 to M9)

In comparison to M2, the four backflow model runs (M6-M9) have floodplain water levels that are both lower than the levee (M6 and M7) and higher than the levee (M8 and M9). The model results show that these differences in floodplain water level have a pronounced influence

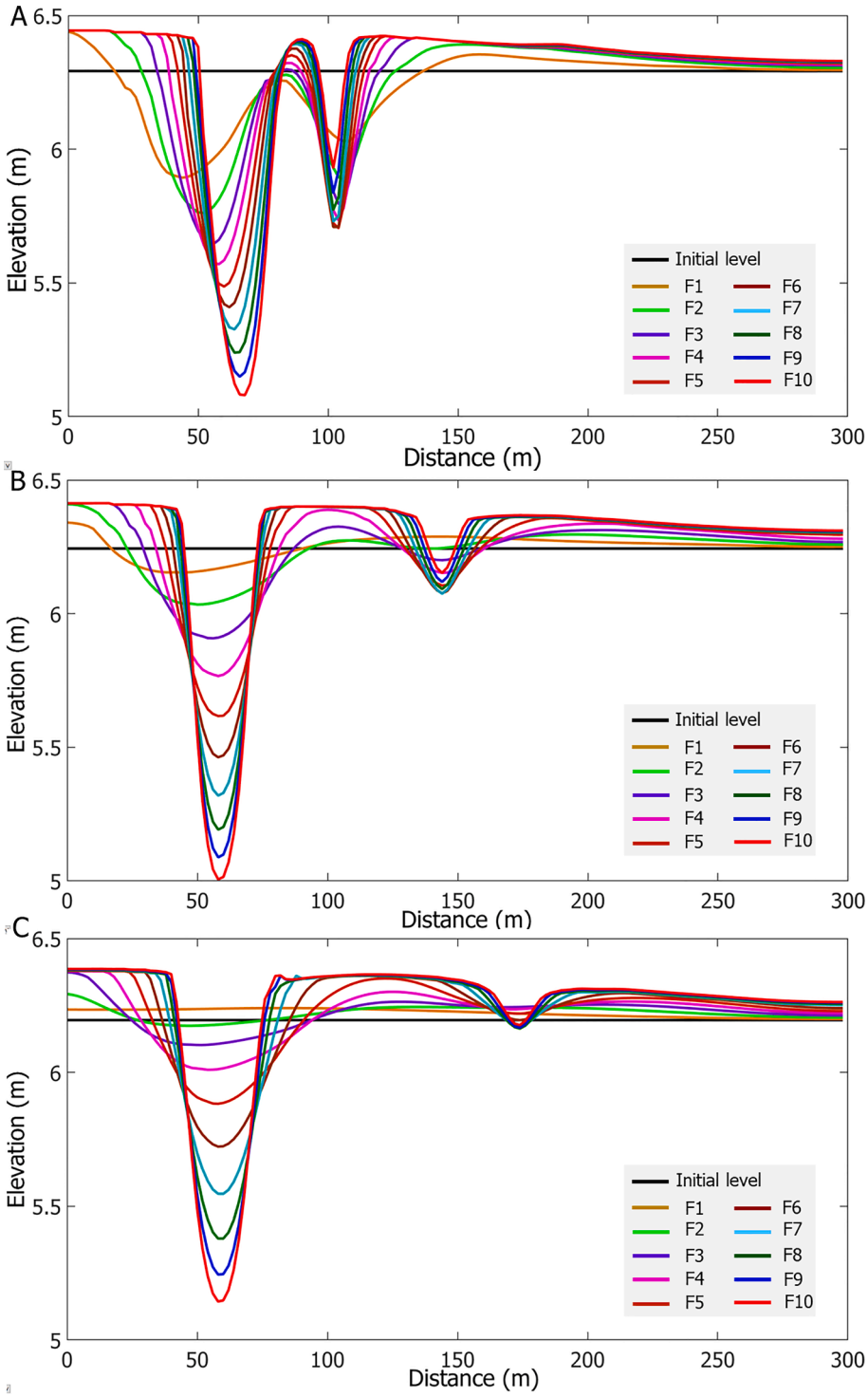

Fig. 6. Three floodplain topographic profiles at A) 200 m, B) 250 m and C) 300 m from the trunk channel (see Fig. 5A for location) for model run M2. F1 through F10 refer to the 1st flood cycle through the 10th flood cycle.

on backflow processes and associated crevasse splay morphodynamics (Fig. 9; Fig. 10).

In models M6 and M7, the trunk channel levee is breached, leading to development of a PSC in similar fashion to that occurring during model run M2, especially in the proximal and medial parts where depths are similar (Fig. 9A-B; Fig. 10). In M6 and M7, a minor SSC branches from the proximal part of the PSC (Fig. 10), but shallows through the flood cycles owing to infilling (Fig. 9D-F).

The areal extent of the PSC, and to some extent the SSC, is large in model runs M6 and M7 in comparison with subsequent backflow model runs M8 and M9 where floodplain water levels are higher (Fig. 10). In M8, two separate crevasse splay channels with similar widths develop, one adjacent to the upstream part of the trunk channel (the PSC), and one farther downstream (the SSC). In M9, the two splay channel widths are more dissimilar, and the SSC is shorter (Fig. 10). In both M8 and M9, the PSC is shallower and shorter compared with the PSC forming in model runs with lower floodplain water levels (Fig. 9A-C; Fig. 10). In contrast to these other model runs, the SSC in model runs M8 and M9

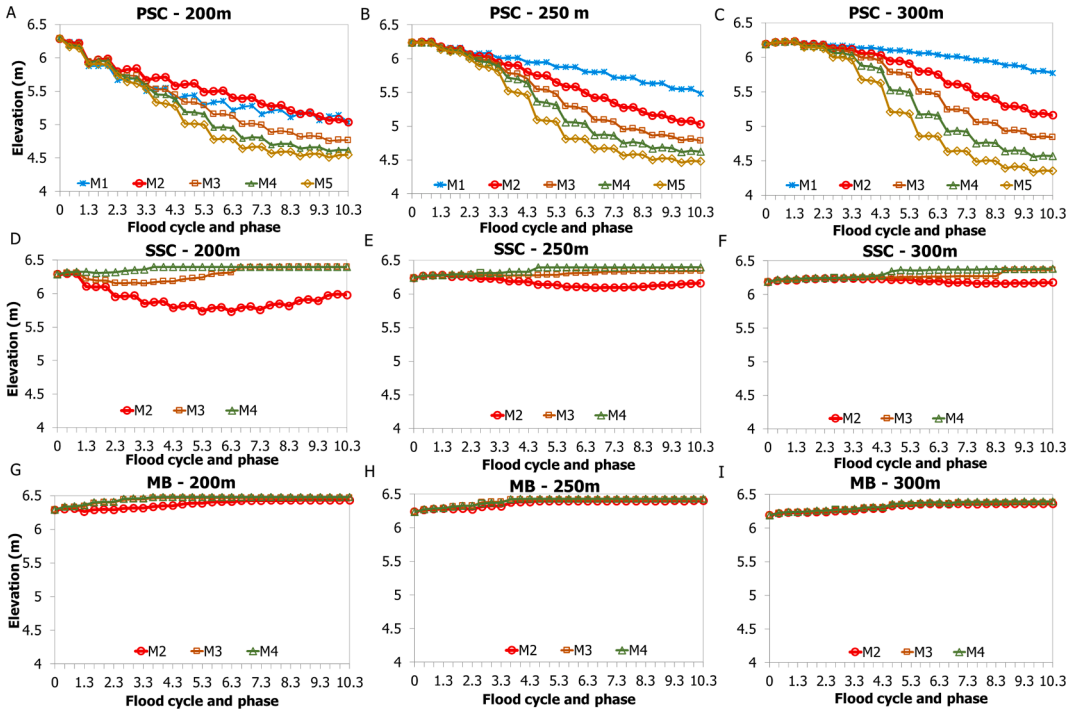

Fig. 7. Elevations of different geomorphological and sedimentary elements for the 10 flood cycles, and the three phases within each cycle, for each of the discharge model runs (M1-M5): PSC: primary splay channel; SSC: secondary splay channel; MB: middle bar. The locations of the floodplain topographic profiles are shown in Fig. 5A. For PSC and SSC, the profile is measured on their lowest points (i.e. bed level) while for middle bar, the profile is measured is on its highest point (i.e. bar top).

continues to deepen through the 10 flood cycles as a result of pronounced erosion (Fig. 9D-F: SSC), with erosion particularly pronounced in M9 close to the junction with the trunk channel (Fig. 10).

In these backflow models, the areal extent and elevation of the middle bar varies (Fig. 9G-I; Fig. 10), in large part owing to the different sizes and spacings of the PSC and SSC. The middle bar either initially increases in elevation through the first few flood cycles before stabilising (e.g. M6 and M7), or tends to increase in elevation through the ten full flood cycles (e.g. M8 and M9), ultimately reaching elevations higher than in other model runs in the proximal, medial and distal profiles, but with a steeper slope from the trunk channel towards the distal floodplain (Fig. 9G-I; Fig. 10).

5. Interpretation

Our numerical modelling results provide scope for evaluating and extending previous inferences about splay development along the lower Río Colorado that have been derived from field and remote sensing data and modelling approaches (e.g. Donselaar et al., 2013, 2022; Li and Bristow, 2015; van Toorenenburg et al., 2018). In particular, our modelling results provide new, quantified, process-based insights into the relative importance of discharge, floodplain water levels and backflow for crevasse splay morphodynamics.

5.1. The development and influence of crevasse channel bifurcations

Reference model M2 is the only model run where a well-developed, essentially stable, crevasse channel bifurcation (i.e. a PSC with a smaller, branching SSC) develops through the flood cycles (Fig. 8). Other model runs with different discharges and/or different floodplain water levels lead to the development of one dominant splay channel (PSC only – M1, M3 to M7) or to two separate crevasse splay channels (PSC and separate

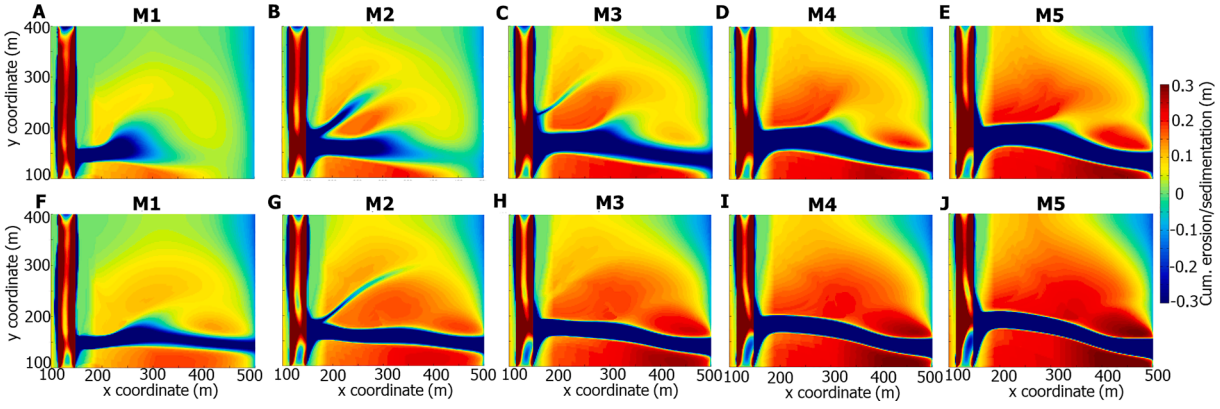

Fig. 8. Comparison of patterns of cumulative erosion and sedimentation across the full model domain for the five discharge model runs (M1-M5) between: A)-E) the end of the 5th flood cycle; and F)-J) the end of the 10th flood cycle.

SSC – see M8 and M9) (Fig. 8; Fig. 10).

In model run M2, soon after the start of flooding along the trunk channel, flow and sediment is diverted to the floodplain as a consequence of levee breaching in the upstream part of the reach (Fig. 8; Fig. 11). Relatively high flow velocities and resulting bed shear stresses through the levee breach in the upstream part of the reach (Fig. 11A-B) promote development of a distinct crevasse channel, with the eroded sediment initially being deposited near the crevasse apex. During the peak of the first flood cycle, flow velocities and maximum bed shear stresses are highest in the floodplain near the crevasse opening, particularly along two main paths that trend obliquely basinward (see arrows in Fig. 11B), resulting in net erosion and sediment dispersal. Flow velocity and shear stress decrease downvalley and laterally across the floodplain (Fig. 11A-B), which leads to widespread sediment deposition, including on prominent bars adjacent to the crevasse (Fig. 11C-D).

The topographic relief created during the first flood peak (phase 1) exerts a fundamental influence on the backflow (phase 3) that occurs as the first flood peak wanes and during which much erosion occurs. During waning flow, discharge in the trunk channel decreases and water level drops but the floodplain water level remains relatively high owing to the enforced residual overbank flow. Consequently, water drains back to the trunk channel (Fig. 12A-C), focusing on the two paths where flow velocities and maximum bed shear stresses were highest during the prior peak flood (Fig. 11A-B; Fig. 12A-C). These two backflow paths are characterized by high flow velocities and maximum bed shear stresses, which leads to further erosion and the lowering and deepening of the crevasse channels, particularly close to the junction with the trunk channel (Fig. 12D-F; Fig. 13A).

By contrast, flow velocities decrease at the junction with the trunk channel (Fig. 12D), with sediment deposition leading to the formation of a reflux lobe (Fig. 13A). The modelling results show that subsequent flood cycles (outflow and backflow) tend to accentuate the floodplain topography established during this first flood event, with the PSC gradually incorporating the offtake of the SSC as the crevasse splay complex develops (Fig. 5).

These simulated erosional and depositional dynamics in model run M2 correspond with previous field and remote sensing observations of some large splay complexes along the Río Colorado (e.g. Fig. 1E-F; Fig. 13B-E), which show that erosion may initiate knickpoints at the junction between different order splay channels or at the junction between the crevasse channel and the trunk channel (cf. Donselaar et al., 2013, their Fig. 15E-F; van Toorenenburg et al., 2018, their Fig. 7C and Fig. 13). Knickpoint migration in subsequent floods may result in knickpoint coalescence, giving rise to extensive, headward eroding channel networks. Similarly, our model results showing the development of reflux lobes (e.g. Fig. 1E-F and Fig. 13B-C, E) correspond with previous field and remote sensing observations (Donselaar et al., 2013, their Fig. 15D-E; Li and Bristow, 2015, their Fig. 17; van Toorenenburg et al. 2018, their Fig. 7A and Fig. 8). The modelling results also demonstrate how reflux lobes tend to form towards the end of each flood event but are eroded in the subsequent flood event and so do not persist as stable, channel features (cf. van Toorenenburg et al., 2018).

5.2. *Channel-floodplain interactions during floods (discharge models)*

Similar to model run M2, in the other discharge model runs (M1, M3 to M5), the first flood (phase 1) tends to establish the floodplain topography that fundamentally influences crevasse splay morphodynamics in the subsequent backflow (phases 2 and 3), with this developing topography then influencing later flood cycles (Fig. 14). Even in the lowest discharge model run (M1, 50 m^3/s), the first flood cycle is sufficient to initiate overbank flow, and also some limited levee breaching and crevasse channel erosion (Fig. 14A). As we used a 2D depth-averaged flow equation in our Delft3D simulations, the typically vertically stratified sediment concentrations in river flows means that the upper water column remains relatively sediment free (cf. Slingerland and Smith, 1998; Meselhe et al., 2012), and so only limited sediment is transferred to the floodplain (Fig. 14A). As discharge increases from M1 to M5, however, increasing volumes of overbank flow are coupled with higher overbank flow velocities and shear stresses, leading to increases

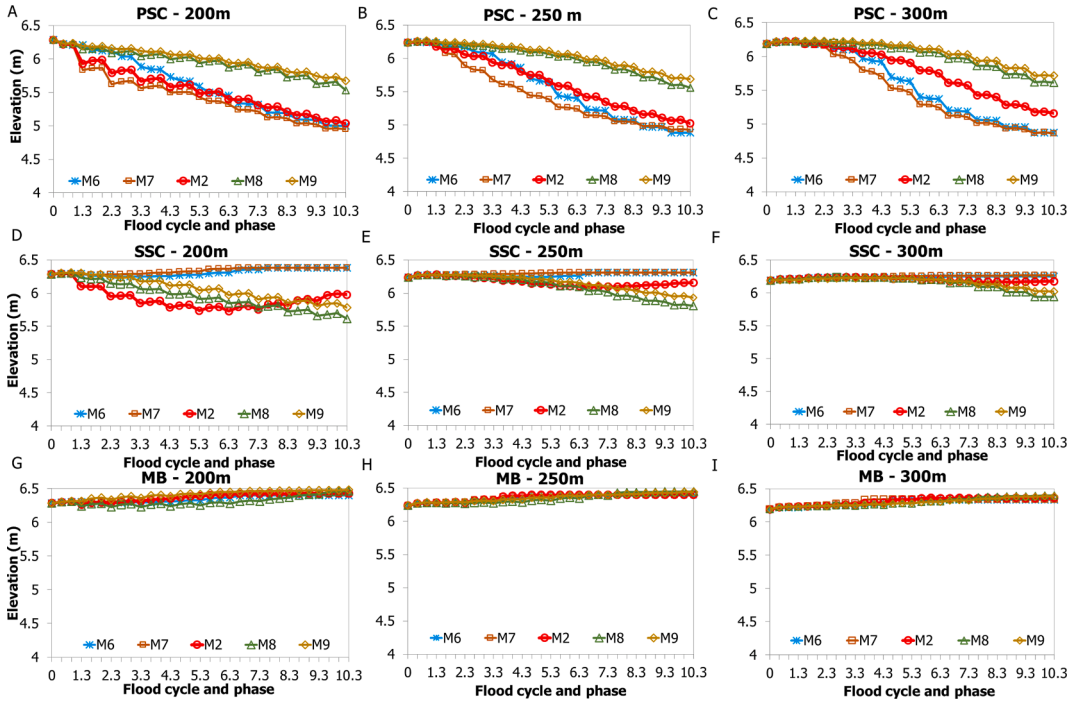

Fig. 9. Elevations of different geomorphological and sedimentary elements for the 10 flood cycles, and the three phases within each cycle, for each of the backflow model runs (M6, M7, M2, M8, M9): PSC: primary splay channel; SSC: secondary splay channel; MB: middle bar. The locations of the floodplain topographic profiles are shown in Fig. 5A. For PSC and SSC, the profile is measured on their lowest points (i.e. bed level) while for middle bar, the profile is measured is on its highest point (i.e. bar top).

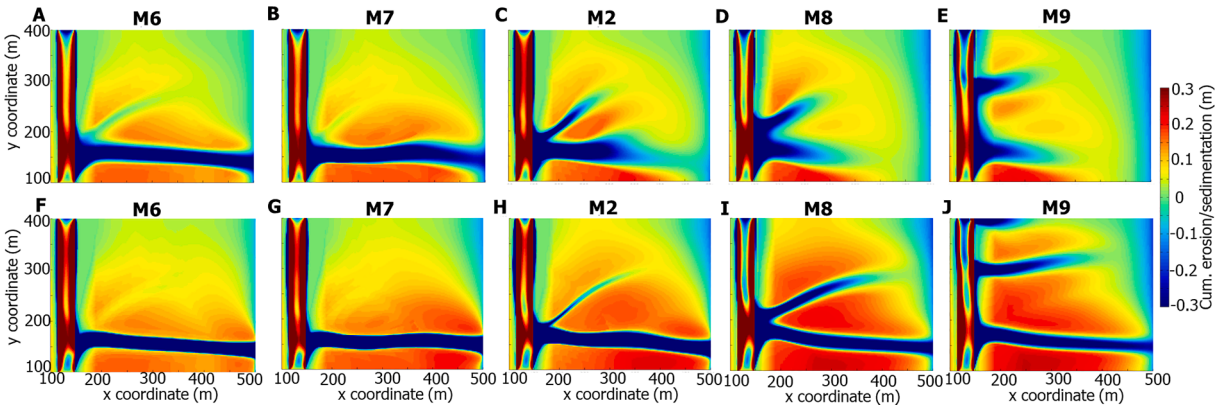

Fig. 10. Comparison of patterns of cumulative erosion and sedimentation across the full model domain for the five backflow model runs (M6, M7, M2, M8, M9) between: A)-E) the end of the 5th flood cycle; and F)-J) the end of the 10th flood cycle.

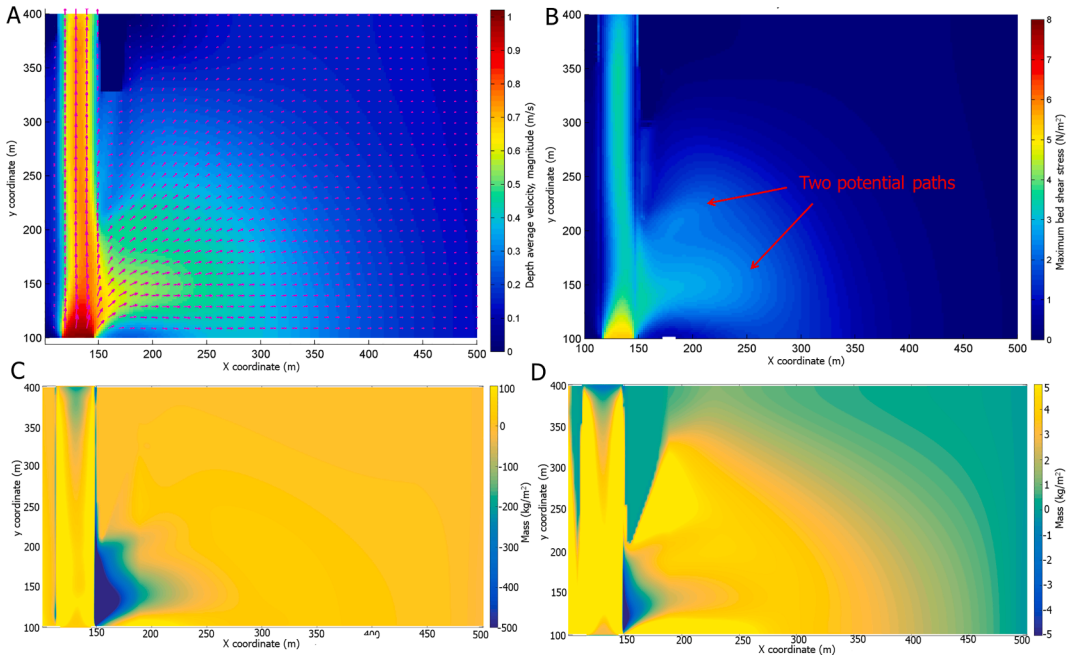

Fig. 11. Maps for peak flow (phase 1) of the first flood cycle of model run M2, showing the distribution of: A) depth-averaged flow velocity; B) maximum bed shear stress; C) sand mass gain/loss; and D) silt mass gain/loss.

in the lateral extent of levee breaching and crevasse channel erosion (Fig. 14B-C). In addition, increasing volumes of sediment are transferred to and across the floodplain, leading to formation of depositional bars. For instance, the formation of an upstream bar, middle bar, and downstream bar in model runs M2 and M3 (Fig. 5; Fig. 8) is a result of the rapid flow expansion that occurs in the transition from relatively confined flow in a crevasse to unconfined overbank flow (cf. Edmonds and Slingerland, 2007). For larger peak discharges (model runs M4 and M5), the PSC deepens and captures an increasing proportion of the flow emanating from the trunk channel (Fig. 8). Consequently, less overbank flow goes through the SSC (Fig. 8), which leads to decreasing flow velocities and sediment deposition. These processes lead to narrowing, shallowing and eventual infilling of the SSC (Fig. 8). This illustrates a more general point: namely, that as increasing amounts of sediment are transferred onto and across the floodplain in an increasingly dominant PSC (Fig. 8), many topographic lows on the more medial and distal parts of the floodplain tend to be filled, locally blocking potential pathways for backflow to the trunk channel after the flood peak has passed (Fig. 14).

5.3. *Backflow processes and their impacts on crevasse morphodynamics*

Similar to model run M2 (see Section 5.1), in the other backflow model runs (M6, M7, M8, M9), the more rapidly decreasing water levels in the trunk channel after the passage of the flood peak create steep local water surface gradients, inducing backflow from the floodplain towards the trunk channel. This backflow tends to be routed through any pre-existing splay channels, commonly inducing erosion near the junction with the trunk channel and forming reflux lobes (Fig. 12; Fig. 13).

A key issue, however, is the extent to which floodplain inundation and backflow accelerate crevasse splay development. In our study, backflow model runs with floodplain water levels that are higher than the levee elevation (i.e. M8, M9) induced return flow to the trunk channel along a greater length of the modelled reach, some of which leads to development of crevasse channels (i.e. the SSCs) that are separate from the area of levee breaching that occurred early in the model runs (Fig. 10D-E). Nevertheless, our modelling results reveal that these high floodplain water levels do not necessarily mean high rates of crevasse channel development across the floodplain. For example, in M8

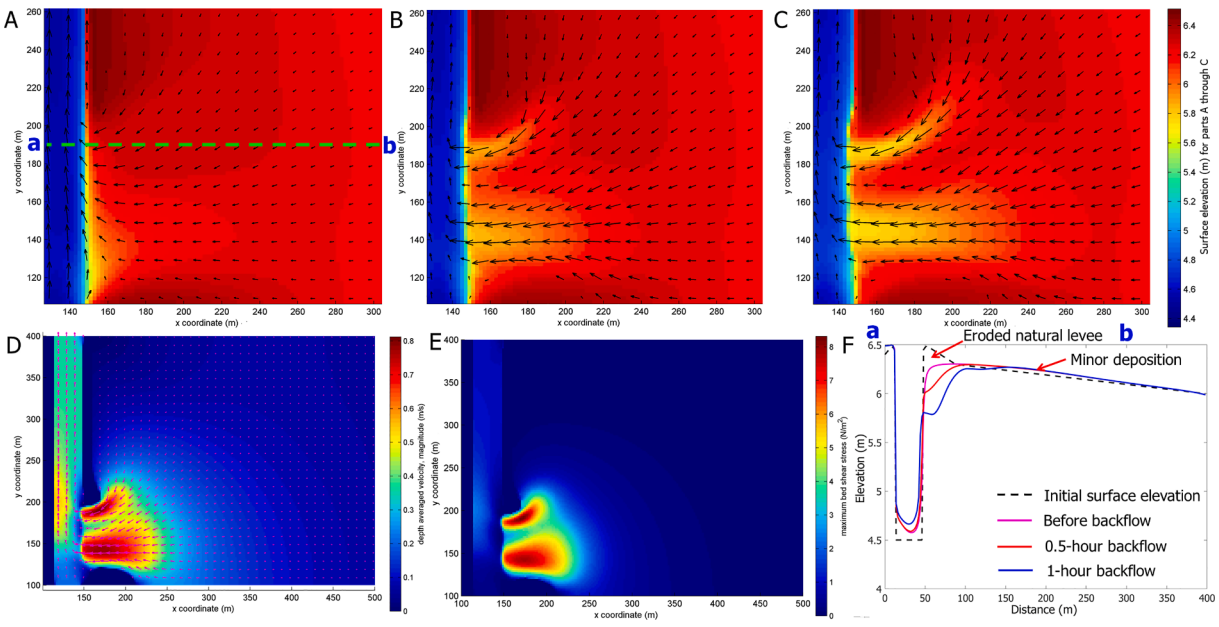

Fig. 12. Maps for backflow (phase 3) of the first flood cycle of model run M2, showing: A)-C) changes in surface elevation in the upstream trunk channel and adjacent floodplain as backflow proceeds; D) the distribution of depth-averaged flow velocity; and E) the distribution of maximum bed shear stress. In A) through D), proportional arrows indicate the relative magnitude of flow velocity. F) Cross-floodplain profiles taken at various stages during backflow at a downstream distance of 190 m perpendicular to the trunk channel (see the location of transect a-b in part A).

and M9, the more downstream crevasse channels (i.e. the SSCs) that are initiated mainly by the higher volumes of backflow, tend to develop at a similar rate compared to the upstream crevasse channels (the PSCs) that are driven by a combination of outflow during peak floods and backflow during waning flow (Fig. 10D-E). The similar development rates of these different crevasse channels, despite different combinations of hydrological drivers, possibly can be attributed to the interaction between outflow and backflow processes. Though the upstream crevasse channels (PSC) receive substantial outflow from the trunk channel, these flows may decelerate under conditions of high floodplain water levels, with a corresponding reduction in erosion. By the same token, the higher floodplain water levels drive more active backflow processes, resulting in widening and deepening of downstream crevasse channels (SSCs) that initially do not receive substantial outflow from the trunk channel.

In fact, our modelling results demonstrate that crevasse channels tend to extend faster across the floodplain when floodplain water levels are lower; driven by strong outflow and proximal erosion, sediment tends not to be deposited on levees but is delivered further onto the floodplain (Fig. 10 – M6, M7). Similar to model run M2, in model runs M6 and M7, one crevasse channel becomes dominant and extends beyond the model domain (Fig. 10), suggesting the potential for some crevasse channels to develop into avulsion pathways that ultimately lead to more profound lateral redistribution of water and sediment (cf. Li et al., 2019).

6. Discussion

Our results and interpretations both support and significantly extend previous inferences about splay development along the lower Río Colorado made by Donselaar et al. (2013, 2022), Li and Bristow (2015), and van Toorenenburg et al. (2018) but also provide scope for comparison with the processes of splay formation along other dryland rivers. In addition, our findings provide insights into the limitations and potential of numerical modelling of splay development.

6.1. Comparisons to splay formation along other dryland rivers

Splays are common features of the lower reaches of ephemeral rivers in endorheic basins, both where riparian vegetation is present (e.g. Tooth, 1999a, b, 2000; 2005; Lang et al., 2004; Fisher et al., 2008; Millard et al., 2017) and largely absent (e.g. Li et al., 2014; Ielpi, 2018; Ielpi and Lapôtre, 2019a). From these settings, however, there are relatively few detailed data on the controls, patterns, processes and rates of splay development.

One exception is provided by Tooth's (2005) field investigations of three ephemeral rivers in arid central Australia, where splays have developed on the outside of channel bends or on straight reaches, despite well-developed bankline vegetation (principally *Eucalyptus* spp.). Splays on the lower Sandover, Sandover-Bundey and Woodforde rivers vary from small, lobate or tongue-shaped features < 1 km long, to larger, elongate features up to ~ 4 km long, and are supplied with rare floodwater and sand and minor gravel through well-defined breaches in the upper parts of the trunk channel banks or levees. In these central Australian channels, splays initially develop when overbank flow initiates a bank/levee breach and scours the floodplain surface, typically in a direction perpendicular to the trunk channel. Subsequent overbank flows further deepen the initial breach, increasing flow and bedload supply from the trunk channel, which in some instances is routed through a primary splay channel on the proximal floodplain and a network of secondary splay channels and bars on the medial and distal floodplain. Some splays remain elevated above the trunk channel but others continue to deepen, increasing the flow and bedload supply during floods. Some may also extend longitudinally, gradually adopting a more elongate form and commonly re-orienting to run subparallel to the trunk channel as a single channel. Once level with the trunk channel bed, these latter types of splays are best termed distributary channels, because they divert water and sediment even during low-magnitude flood events (Tooth, 2005). Continued development of a distributary channel ultimately may lead to an avulsion, with flow and sediment transport switching to the distributary and the former trunk channel being abandoned. In these central Australia rivers, overbank floods in the lower reaches are infrequent (once every 1–2 years or less), so splays and distributary channels develop relatively slowly over many decades (Tooth, 2005).

Despite differences in the degree of riparian vegetation, sediment calibre, and rates of development, splay channels along the lower

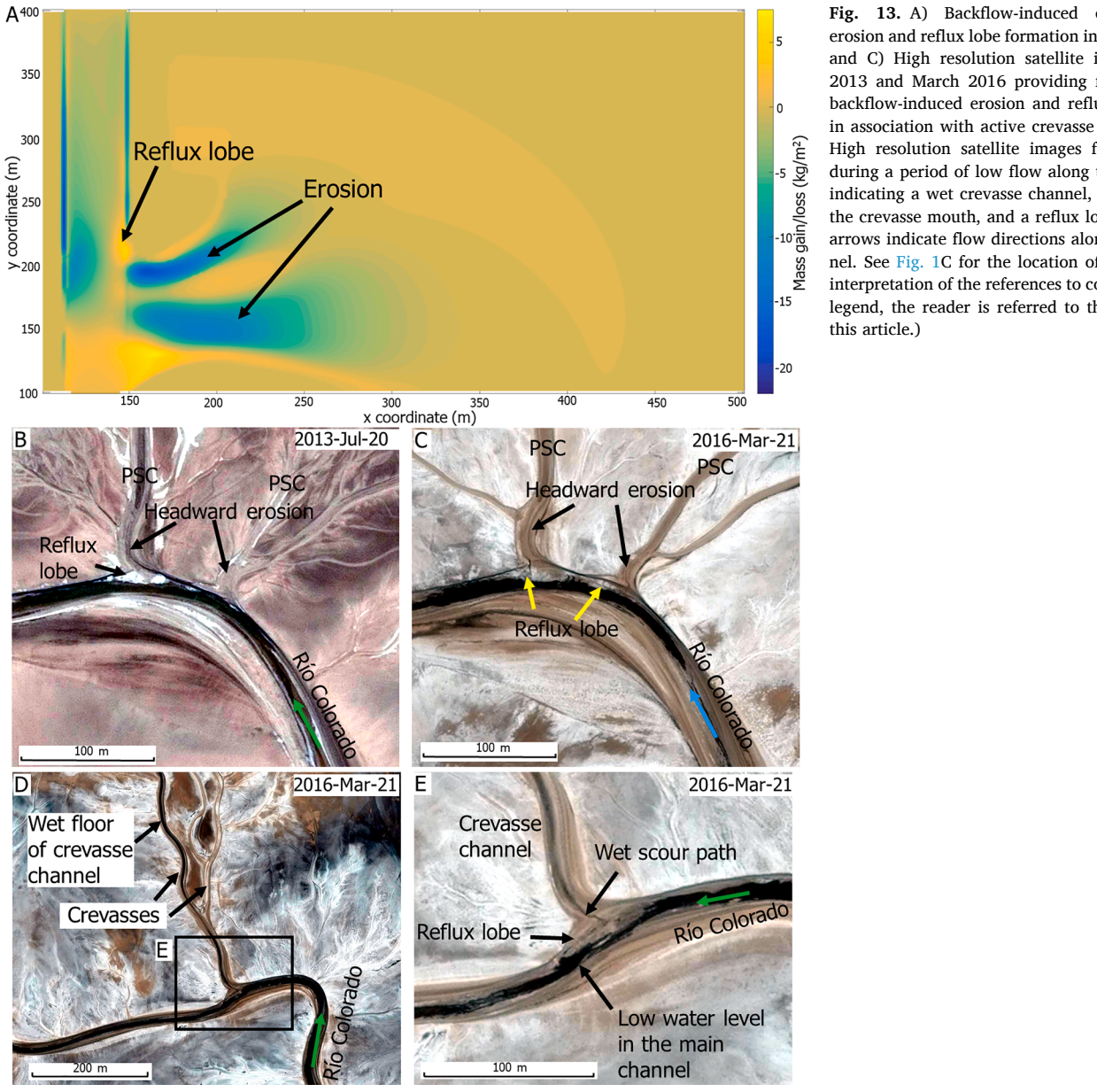

Fig. 13. A) Backflow-induced crevasse channel erosion and reflux lobe formation in model run M2. B) and C) High resolution satellite images from July 2013 and March 2016 providing field evidence for backflow-induced erosion and reflux lobe formation in association with active crevasse splays. D) and E) High resolution satellite images from March 2016 during a period of low flow along the main channel, indicating a wet crevasse channel, a scour path near the crevasse mouth, and a reflux lobe. Green or blue arrows indicate flow directions along the main channel. See Fig. 1C for the location of the images. (For interpretation of the references to colour in this figure legend, the reader is referred to the web version of this article.)

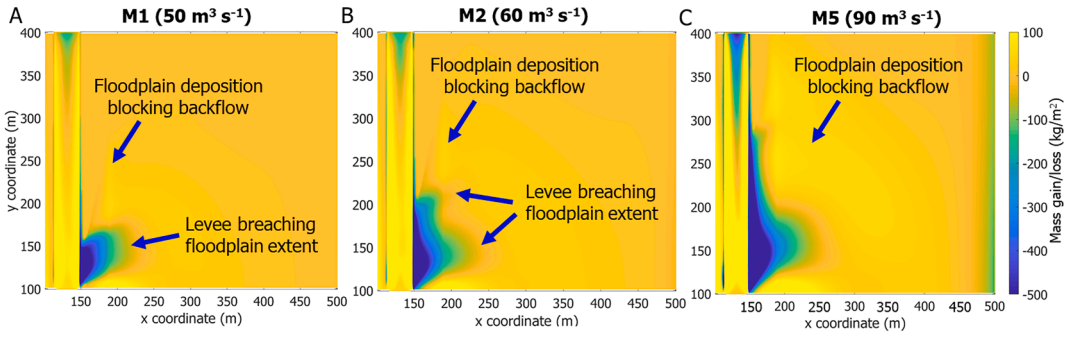

Fig. 14. Comparison of net erosion and deposition (i.e. mass gain/loss) for phase 1 of the first flood cycle (i.e. before backflow) in different discharge model runs.

reaches of these central Australian rivers clearly have many morphological similarities with the Río Colorado splays. But what about the hydrological conditions under which these splays develop? Flood hydrological conditions in the remote central Australian channels are not well known, but the field evidence (e.g. orientation of flattened grasses, flood debris, local bedforms) suggests that prolonged high floodplain water levels and backflow after the passage of peak stage is not a major factor (Tooth, 2005). This suggests that conditions similar to our

discharge model runs M1-M5 (Fig. 8) with their dominance of outflow are probably most prevalent. Along these rivers, shorter, commonly bifurcating, lobate or tongue-shaped splays may develop under conditions most similar to model runs M1 or early stage M2 or M3, and larger, elongate splays with a dominant channel may develop under conditions most similar to model runs M3 to M5 (Fig. 8).

By contrast, flood hydrological conditions along the topographically complex lower Río Colorado are highly spatially non-uniform, with the widespread distribution of active and abandoned fluvial landforms significantly influencing the patterns, depths and durations of overbank flows (Li et al., 2018). While some parts of the floodplain are relatively free draining, prolonged high floodplain water levels (overbank depths up to ~ 0.5 m) may be promoted in localised topographic depressions (e.g. within palaeochannels and cutoffs, or between the elevated topography created by palaeochannel belts or older crevasse splay complexes), leading to strong backflow after peak stage has passed. Along the Río Colorado, therefore, shorter splays may develop under conditions that either involve limited outflow (model runs M1 and early stage M2 or M3) or high floodplain water levels with pronounced backflow (M8, M9) (Figs. 8 and 10). Longer splays with a dominant channel may develop under conditions involving a mix of strong outflow and moderately high floodplain water levels with moderate backflow (later stage M2 and M3, M4 to M7) (Figs. 8 and 10).

6.2. Evaluation in relation to other splay modelling studies

Our interpretations of the hydrological conditions under which crevasse splays develop along the Río Colorado and the central Australian rivers is supported by previous splay modelling results, most notably Millard et al. (2017). As part of an investigation into floodbasin hydrological and sediment supply controls on crevasse splay size, Millard et al. (2017) used aerial photographs to remap and quantify the dimensions of splays along the lower Sandover River, first described by Tooth (2005). Along with comparable data from splays developed along the humid region Columbia and Saskatchewan rivers, Millard et al. (2017) then conducted a targeted numerical modelling study using Delft3D. While their model setup has some noticeable differences from that adopted in our study (see Sections 2 and 3), broad comparisons can still be made.

Most significantly, Millard et al. (2017) concluded that splay size (length, area) does not always scale directly with channel size or discharge and that hydrodynamic factors – principally sediment size and floodplain drainage conditions – play a significant role in determining whether or not large, floodplain-filling splays develop. For example, in rivers carrying sufficient volumes of coarse suspended sediment, floodplain drainage conditions determine the shape and extent of splay deposition. Widespread splay deposits can form if floodplain conditions promote strong cross-floodplain water surface slopes (i.e. 'drained floodplains' without significant ponding); in some cases, these conditions may also facilitate bedload transport across floodplains (cf. Pizzuto et al., 2008). By contrast, when cross-floodplain water surface gradients are far lower than downstream channel slopes (i.e. 'ponded floodplains'), thick splay deposits may accumulate adjacent to the crevasse opening but sediment dispersal and widespread aggradation farther from the channel will be limited (Millard et al., 2017). Together, these model results help to explain the field evidence from their study rivers: Saskatchewan River splays that develop under relatively free-draining floodplain conditions tend to be fewer in number but larger, and divert more sediment than the more numerous, smaller Columbia River splays that develop under more ponded floodplain conditions. This is similar to the modelling results from our study, which show clearly that high floodplain water levels ('ponding') restrict the spatial extent (length, area) of splays (Fig. 10), probably owing to deceleration of outflow as slow moving or standing floodplain water is encountered.

Interestingly, Millard et al. (2017) interpreted the Sandover River data as more similar to the Saskatchewan data in terms of splay area and extent but as falling between the Columbia and Saskatchewan data in terms of splay occurrence and splay-covered floodplain fraction. While a lack of discharge data meant that Millard et al. (2017) explicitly excluded the Sandover data from their more detailed analyses of discharge-splay sediment volume, overall their results would suggest that the Sandover – and by implication other similar central Australian rivers – experience flood hydrological conditions that are relatively free-draining and do not involve widespread or prolonged ponding. This corresponds with the earlier field observations and interpretations of Tooth (2005) and the interpretations resulting from a comparison of the central Australian splays with our Río Colorado modelling results (Section 6.1).

6.3. Further model developments

Similar to previous modelling approaches that have made simplifying assumptions in order to isolate some of the key factors influencing splay development (e.g. Slingerland and Smith, 1998; Millard et al., 2017; Nienhuis et al., 2018), our model setup was designed primarily to investigate the role of hydrological controls (specifically the relative roles of discharge, floodplain water levels and backflow) in the development of splays along a simple channel-floodplain reach of the lower Río Colorado. As such, while our results and interpretations provide valuable insights to support and extend previous field, remote sensing and conceptual model inferences about splay development along the Río Colorado in particular, but also dryland splays more generally, many uncertainties remain. Similar to Millard et al. (2017), we draw attention to the need for further studies of coupled channel-floodplain systems that explore more fully the morphodynamic feedbacks and sensitivities associated with different mixes of hydrological, sediment supply and floodplain topographic conditions.

Various lines of investigation can be suggested as priorities for future investigations of splay development along the lower Río Colorado and other dryland rivers. First, given the rapid rise of stage that is characteristic of floods in ephemeral rivers in particular, more attention needs to be given to the potential importance of this transient part of the flood wave in initiating and promoting crevasse splay development (cf. Millard et al., 2017), particularly in channels where ramping of coarse-grained (e.g. sand, minor gravel) bedload up elevated bars is a key component of the sediment supply to splays (see Tooth, 2005). Second, more attention could be focused on the role of varied sediment supply across a range of grain size conditions; for instance, the Río Colorado is relatively fine-grained with sediment typically supplied annually to splays, whereas in the central Australian rivers sediment is coarser grained and supplied more infrequently to developing splay channels. Third, on highly complex floodplains like the Río Colorado, model setups could explore the role of prior rainfall and pre-existing floodplain topography (e.g. as created by palaeochannels, cutoffs, older splay complexes, or erosion cells – see Li et al., 2019) in influencing hydrological conditions, particularly the critical balance between relatively free draining and more ponded conditions that have such a strong influence on splay channel morphodynamics (Figs. 8 and 10). On the Río Colorado and other similar rivers, there is also scope for making use of improved insights into the spatial and temporal variations in hydrological conditions within and between floods that are resulting from advances in the use of repeat, very high resolution satellite images and improved processing techniques (Li et al., 2018).

Finally, while not a focus of this study, further attention could also be directed to the relative importance of crevasse splay development in promoting avulsions on the Río Colorado and other dryland rivers. Previous splay modelling studies (e.g. Slingerland and Smith, 1998; Hajek and Edmonds, 2014; Millard et al., 2017) have considered the relation between crevasse splay development and the progradational avulsion style (see also Slingerland and Smith, 2004). While beyond the scope of our study, some of the model outputs (e.g. Figs. 8 and 10) suggest that certain hydrological conditions are more favourable for the

development of a dominant splay channel that over time could lead to diversion of increasing volumes of flow and sediment from the trunk channel and ultimately result in avulsion (cf. Donselaar et al., 2013, 2022; van Toorenenburg et al., 2018; Li et al., 2018, 2019). It is worth noting, however, that avulsions on the lower Río Colorado do not necessarily involve splay development; similar to some other dryland rivers (Tooth et al., 2007, 2008; Larkin et al., 2017), incisional avulsions involving floodplain scour and incision (e.g. through development of headcutting channels or coalescence of erosion cells) and/or reoccupational avulsions involving reworking of older palaeochannels may be of equal or greater significance in redistributing water and sediment (Li et al., 2019). Indeed, on distributive fluvial systems like the lower Río Colorado, where abundant palaeochannels, cutoffs, older splay complexes, and erosion cells create highly complex floodplain topography, splays that initially develop as a result of splay progradation are increasingly likely to encounter headcutting channels, erosion cells or palaeochannels as they lengthen, perhaps leading to a change over time in the dominant avulsion style.

7. Conclusions

Present knowledge of the geomorphology and sedimentology of dryland river floodplains is incomplete, with the characteristics of overbank deposits such as splays typically being poorly documented in comparison with channel forms and deposits. Over recent years, however, field, remote sensing and modelling studies of the non-vegetated, ephemeral Río Colorado have contributed significant information, particularly because regular flooding drives cascades of pronounced, widespread channel-floodplain changes on far shorter timescales than is typical in many other dryland systems. This study has shown how process-based modelling using Delft3D can provide additional insights into splay development, complementing and significantly extending previous findings, both on the lower Río Colorado but also along dryland rivers more generally.

Our modelling results show that discharge, floodplain water levels and backflow all exert significant influences on splay development and potential wider channel-floodplain dynamics. Simulated results reveal that increases in discharge lead to more rapid splay sedimentation and stabilization of a single crevasse channel. Increases in floodplain water level result in shorter but wider splays. High water levels restrict the spatial extent of splays, probably owing to deceleration of outflow as slow moving or standing floodplain water is encountered, but these conditions promote separate crevasse channel formation farther downstream as backflow breaches the trunk channel levee during falling stage. A key objective in future research into dryland splays will be to couple additional field and remote sensing observations with modelling studies that incorporate a wider range of hydrological, sediment supply, and floodplain topographic conditions. This will help to build more comprehensive models of splay development that can advance knowledge of the spatial and temporal controls, patterns, processes and rates of channel-floodplain development in dryland endorheic basins.

CRediT authorship contribution statement

Jiaguang Li: Conceptualization, Methodology, Investigation, Writing - original draft, Writing - review & editing. **Helena van der Vegt:** Methodology, Writing – review & editing. **Joep E.A. Storms:** Methodology. **Stephen Tooth:** Writing – review & editing.

Declaration of Competing Interest

The authors declare that they have no known competing financial interests or personal relationships that could have appeared to influence the work reported in this paper.

Data availability

Data will be made available on request.

Acknowledgements

This research was supported by: the National Natural Science Foundation of China (No. 42172133, No. 41972114, No. 41602121); Wuhan Applied Foundational Frontier Project (No. 2020020601012281); and the Fundamental Research Funds for the Central Universities, China University of Geosciences, Wuhan (No. CUG2021206). JL thanks Dr. Peng Yao and Liang Li for the constructive discussion and data processing about the research. We thank the two anonymous for comments and questions that enabled us to clarify our arguments.

References

Aslan, A., Autin, W.J., Blum, M.D., 2005. Causes of river avulsion: Insights from the Late Holocene avulsion history of the Mississippi River, U.S.A. J. Sediment. Res. 75, 650–664. https://doi.org/10.2110/jsr.2005.053.

Bjerklie, D.M., 2007. Estimating the bankfull velocity and discharge for rivers using remotely sensed river morphology information. J. Hydrol. 341 (3-4), 144–155.

Bridge, J.S., 2003. Rivers and Floodplains: Forms, Processes and the Sedimentary Record. Blackwell Publishing, Oxford, UK.

Bristow, C.S., Skelly, R.L., Ethridge, F.G., 1999. Crevasse splays from the rapidly aggrading, sand-bed, braided Niobrara River, Nebraska: Effect of base-level rise. Sedimentology 46, 1029–1047. https://doi.org/10.1046/j.1365-3091.1999.00263.x.

Buehler, H.A., Weissmann, G.S., Scuderi, L.A., Hartley, A.J., 2011. Spatial and temporal evolution of an avulsion on the Taquari River distributive fluvial system from satellite image analysis. J. Sediment. Res. 81, 630–640. https://doi.org/10.2110/jsr.2011.040.

David, S.R., Czuba, J.A., Edmonds, D.A., 2018. Channelization of meandering river floodplains by headcutting. Geology 47, 15–18. https://doi.org/10.1130/G45529.1.

Donselaar, M.E., Gozalo, M.C.C., Moyano, S., 2013. Avulsion processes at the terminus of low-gradient semi-arid fluvial systems: Lessons from the Río Colorado, Altiplano endorheic basin, Bolivia. Sediment. Geol. 283, 1–14. https://doi.org/10.1016/j.sedgeo.2012.10.007.

Donselaar, M.E., Cuevas Gozalo, M.C., van Toorenenburg, K.A., Wallinga, J., 2022. Spatio-temporal reconstruction of avulsion history at the terminus of a modern dryland river system. Earth Surf. Process. Landforms 47, 1212–1228. https://doi.org/10.1002/esp.5311.

Edmonds, D.A., Slingerland, R.L., 2007. Mechanics of river mouth bar formation: Implications for the morphodynamics of delta distributary networks. J. Geophys. Res. Earth Surf. 112, 1–14. https://doi.org/10.1029/2006JF000574.

Edmonds, D.A., Slingerland, R.L., 2008. Stability of delta distributary networks and their bifurcations. Water Resour. Res. 44, 1–13. https://doi.org/10.1029/2008WR006992.

Engelund, F., Hansen, E., 1967. A Monograph on Sediment Transport in Alluvial Streams. Copenhagen, Denmark.

Fisher, J.A., Krapf, C.B.E., Lang, S.C., Nichols, G.J., Payenberg, T.H.D., 2008. Sedimentology and architecture of the Douglas Creek terminal splay, Lake Eyre, central Australia. Sedimentology 55, 1915–1930.

Florsheim, J.L., Mount, J.F., 2002. Restoration of floodplain topography by sand-splay complex formation in response to intentional levee breaches, Lower Cosumnes River, California. Geomorphology 44, 67–94. https://doi.org/10.1016/S0169-555X(01)00146-5.

Hajek, E.A., Edmonds, D.A., 2014. Is river avulsion style controlled by floodplain morphodynamics? Geology 42, 199–202. https://doi.org/10.1130/G35045.1.

Hajek, E.A., Wolinsky, M.A., 2012. Simplified process modeling of river avulsion and alluvial architecture: Connecting models and field data. Sediment. Geol. 257–260, 1–30. https://doi.org/10.1016/j.sedgeo.2011.09.005.

Ielpi, A., 2018. Morphodynamics of meandering streams devoid of plant life: Amargosa River, Death Valley, California. GSA Bull. 131, 782–802. https://doi.org/10.1130/B31960.1.

Ielpi, A., Lapôtre, M.G.A., 2019. Barren Meandering Streams in the Modern Toiyabe Basin of Nevada, U.S.A., and Their Relevance To the Study of the Pre-vegetation Rock Record. J. Sediment. Res. 89, 399–415. https://doi.org/10.2110/jsr.2019.25.

Ielpi, A., Lapôtre, M.G.A., Veiga, G., 2019. Biotic forcing militates against river meandering in the modern Bonneville Basin of Utah. Sedimentology 66 (5), 1896–1929.

Kleinhans, M.G., Ferguson, R.I., Lane, S.N., Hardy, R.J., 2013. Splitting rivers at their seams: bifurcations and avulsion. Earth Surf. Process. Landforms 38, 47–61. https://doi.org/10.1002/esp.3268.

Lang, S.C., Payenberg, T.H.D., Reilly, M.R.W., Hicks, T., Benson, J., Kassan, J., 2004. Modern analogues for dryland sandy fluvial-lacustrine deltas and terminal splay reservoirs. APPEA J. 44, 329–356.

Larkin, Z.T., Ralph, T.J., Tooth, S., McCarthy, T.S., 2017. The interplay between extrinsic and intrinsic controls in determining floodplain wetland characteristics in the South

African drylands. Earth Surf. Process. Landforms 42, 1092–1109. https://doi.org/10.1002/esp.4075.
Lesser, G.R., Roelvink, J.A., van Kester, J.A.T.M., Stelling, G.S., 2004. Development and validation of a three-dimensional morphological model. Coast. Eng. 51, 883–915. https://doi.org/10.1016/j.coastaleng.2004.07.014.
Lewin, J., Ashworth, P.J., Strick, R.J.P., 2017. Spillage sedimentation on large river floodplains. Earth Surf. Process. Landforms 42, 290–305. https://doi.org/10.1002/esp.3996.
Li, J., Bristow, C.S., 2015. Crevasse splay morphodynamics in a dryland river terminus: Río Colorado in Salar de Uyuni Bolivia. Quat. Int. 377, 71–82. https://doi.org/10.1016/j.quaint.2014.11.066.
Li, J., Donselaar, M.E., Hosseini Aria, S.E., Koenders, R., Oyen, A.M., 2014. Landsat imagery-based visualization of the geomorphological development at the terminus of a dryland river system. Quat. Int. 352, 100–110. https://doi.org/10.1016/j.quaint.2014.06.041.
Li, J., Luthi, S.M., Donselaar, M.E., Weltje, G.J., Prins, M.A., Bloemsma, M.R., 2015. An ephemeral meandering river system: Sediment dispersal processes in the Río Colorado, Southern Altiplano Plateau, Bolivia. Zeitschrift für Geomorphol. 59 (3), 301–317.
Li, J., Yang, X., Maffei, C., Tooth, S., Yao, G., 2018. Applying independent component analysis on Sentinel-2 imagery to characterize geomorphological responses to an extreme flood event near the non-vegetated Río Colorado terminus, Salar de Uyuni, Bolivia. Remote Sens. 10, 725. https://doi.org/10.3390/rs10050725.
Li, J., Tooth, S., Yao, G., 2019. Cascades of sub-decadal, channel-floodplain changes in low-gradient, non-vegetated reaches near a dryland river terminus: Salar de Uyuni, Bolivia. Earth Surf. Process. Landforms 44, 490–506. https://doi.org/10.1002/esp.4512.
Li, J., Grenfell, M.C., Wei, H., Tooth, S., Ngiem, S., 2020a. Chute cutoff-driven abandonment and sedimentation of meander bends along a fine-grained, non-vegetated, ephemeral river on the Bolivian Altiplano. Geomorphology 350, 106917. https://doi.org/10.1016/j.geomorph.2019.106917.
Li, J., Vandenberghe, J., Mountney, N.P., Luthi, S.M., 2020b. Grain-size variability of point-bar deposits from a fine-grained dryland river terminus, Southern Altiplano, Bolivia. Sediment. Geol. 403, 105663 https://doi.org/10.1016/j.sedgeo.2020.105663.
Li, J., Zhao, Y., Bates, P., Neal, J., Tooth, S., Hawker, L., Maffei, C., 2020c. Digital Elevation Models for topographic characterisation and flood flow modelling along low-gradient, terminal dryland rivers: a comparison of spaceborne datasets for the Río Colorado, Bolivia. J. Hydrol. 591, 125617 https://doi.org/10.1016/j.jhydrol.2020.125617.
Li, J., Tooth, S., Zhang, K., Zhao, Y., 2021. Visualisation of flooding along an unvegetated, ephemeral river using Google Earth Engine: Implications for assessment of channel-floodplain dynamics in a time of rapid environmental change. J. Environ. Manage. 278, 111559 https://doi.org/10.1016/j.jenvman.2020.111559.
Li, J., Ganti, V., Li, C., Wei, H., 2022. Upstream migration of avulsion sites on lowland deltas with river-mouth retreat. Earth Planet. Sci. Lett. 577, 117270 https://doi.org/10.1016/j.epsl.2021.117270.
Li, J., 2014. Terminal Fluvial Systems in a Semi-arid Endorheic Basin, Salar de Uyuni (Bolivia). Uitgeverij BOX Press, 's-Hertogenbosch, The Netherlands.
Mertes, L.A.K., Dunne, T., Martinelli, L.A., 1996. Channel-floodplain geomorphology along the Solimões-Amazon River, Brazil. GSA Bull. 108, 1089–1107. doi: 10.1130/0016-7606(1996)108<1089:CFGATS>2.3.CO;2.
Meselhe, E.A., Georgiou, I., Allison, M.A., Mccorquodale, J.A., 2012. Numerical modeling of hydrodynamics and sediment transport in lower Mississippi at a proposed delta building diversion. J. Hydrol. 472–473, 340–354. https://doi.org/10.1016/j.jhydrol.2012.09.043.
Miall, A.D., 1996. The Geology of Fluvial Deposits. Springer, New York.
Millard, C., Hajek, E., Edmonds, D.A., 2017. Evaluating controls on crevasse-splay size: implications for floodplain-basin filling. J. Sediment. Res. 87 (7), 722–739.
Morehead, M.D., Syvitski, J.P., Hutton, E.W.H., Peckham, S.D., 2003. Modeling the temporal variability in the flux of sediment from ungauged river basins. Glob. Planet. Change 39, 95–110. https://doi.org/10.1016/S0921-8181(03)00019-5.
Nienhuis, J.H., Törnqvist, T.E., Esposito, C.R., 2018. Crevasse splays versus avulsions: a recipe for land building with levee breaches. Geophys. Res. Lett. 45, 4058–4067. https://doi.org/10.1029/2018GL077933.
Pizzuto, J.E., Moody, J.A., Meade, R.H., 2008. Anatomy and dynamics of a floodplain, powder river, Montana, U.S.A. J. Sediment. Res. 78, 16–28. https://doi.org/10.2110/jsr.2008.005.
Placzek, C.J., Quade, J., Patchett, P.J., 2013. A 130ka reconstruction of rainfall on the Bolivian Altiplano. Earth Planet. Sci. Lett. 363, 97–108. https://doi.org/10.1016/j.epsl.2012.12.017.
Rahman, M.M., Howell, J.A., MacDonald, D.I.M., 2022. Quantitative analysis of crevasse-splay systems from modern fluvial settings. J. Sediment. Res. 92 (9), 751–774.
Reid, I., Frostick, L.E., 2011. Channel Form, Flows and Sediments in Deserts. In: Thomas, D.S.G. (Ed.), Arid Zone Geomorphology: Process, Form and Change in Drylands. John Wiley & Sons Ltd, Chichester, pp. 301–332.
Sandén, A.B., 2016. Process-based Modelling of a Crevasse Splay. Delft University of Technology. https://doi.org/http://repository.tudelft.nl.
Schuurman, F., Marra, W.A., Kleinhans, M.G., 2013. Physics-based modeling of large braided sand-bed rivers: Bar pattern formation, dynamics, and sensitivity. J. Geophys. Res. Earth Surf. 118, 2509–2527. https://doi.org/10.1002/2013JF002896.
Shen, Z., Törnqvist, T.E., Mauz, B., Chamberlain, E.L., Nijhuis, A.G., Sandoval, L., 2015. Episodic overbank deposition as a dominant mechanism of floodplain and delta-plain aggradation. Geology 43, 875–878. https://doi.org/10.1130/G36847.1.
Slingerland, R., Smith, N.D., 1998. Necessary conditions for a meandering-river avulsion. Geology 26, 435. https://doi.org/10.1130/0091-7613(1998)026<0435:NCFAMR>2.3.CO;2.
Slingerland, R., Smith, N.D., 2004. River avulsion and their deposits. Annu. Rev. Earth Planet. Sci. 32, 257–285.
Smith, N.D., Perez-Arlucea, M., 1994. Fine-grained splay deposition in the avulsion belt of the lower Saskatchewan River, Canada. J. Sediment. Res. B Stratigr. Glob. Stud. 64, 159–168. https://doi.org/10.1306/D4267F7D-2B26-11D7-8648000102C1865D.
Stouthamer, E., 2001. Sedimentary products of avulsions in the Holocene Rhine-Meuse Delta, The Netherlands. Sediment. Geol. 145, 73–92. https://doi.org/10.1016/S0037-0738(01)00117-8.
Toonen, W.H.J., van Asselen, S., Stouthamer, E., Smith, N.D., 2016. Depositional development of the Muskeg Lake crevasse splay in the Cumberland Marshes (Canada). Earth Surf. Process. Landforms 41, 117–129. https://doi.org/10.1002/esp.3791.
Tooth, S., 1999a. Floodouts in central Australia. In: Miller, A.J., Gupta, A. (Eds.), Varieties of Fluvial Form. Wiley, Chichester, pp. 219–247.
Tooth, S., 2000. Downstream changes in dryland river channels: The Northern Plains of arid central Australia. Geomorphology 34, 33–54. https://doi.org/10.1016/S0169-555X(99)00130-0.
Tooth, S., 2005. Splay Formation Along the Lower Reaches of Ephemeral Rivers on the Northern Plains of Arid Central Australia. J. Sediment. Res. 75, 636–649. https://doi.org/10.2110/jsr.2005.052.
Tooth, S., Jansen, J.D., Nanson, G.C., Coulthard, T.J., Pietsch, T., 2008. Riparian vegetation and the late Holocene development of an anabranching river: Magela Creek, northern Australia. Bull. Geol. Soc. Am. 120, 1021–1035. https://doi.org/10.1130/B26165.1.
Tooth, S., Nanson, G.C., 2011. Distinctiveness and diversity of arid zone river systems. In: Thomas, D.S.G. (Ed.), Arid Zone Geomorphology: Process, Form and Change in Drylands. Wiley, pp. 269–300.
Tooth, S., Rodnight, H., Duller, G.A.T., McCarthy, T.S., Marren, P.M., Brandt, D., 2007. Chronology and controls of avulsion along a mixed bedrock-alluvial river. Bull. Geol. Soc. Am. 119, 452–461. https://doi.org/10.1130/B26032.1.
Tooth, S., 1999b. Downstream changes in floodplain character on the Northern Plains of arid central Australia, in: Smith, N.D., Rogers, J. (Eds.), Fluvial Sedimentology VI. International Association of Sedimentologists, Special Publication No. 28, Blackwell Oxford, UK, pp. 93–112.
Tooth, S., 2013. Dryland Fluvial Environments: Assessing Distinctiveness and Diversity from a Global Perspective, in: Shroder, J.F. (Ed. In Chief) and Wohl, E.E. (Ed.), Treatise on Geomorphology. Volume 9: Fluvial Geomorphology. Academic Press, San Diego, CA, pp. 612–644. doi: 10.1016/j.rser.2012.02.011.
van Toorenenburg, K.A., Donselaar, M.E., Noordijk, N.A., Weltje, G.J., 2016. On the origin of crevasse-splay amalgamation in the Huesca fluvial fan (Ebro Basin, Spain): Implications for connectivity in low net-to-gross fluvial deposits. Sediment. Geol. 343, 156–164. https://doi.org/10.1016/j.sedgeo.2016.08.008.
van Toorenenburg, K.A., Donselaar, M.E., Weltje, G.J., 2018. The life cycle of crevasse splays as a key mechanism in the aggradation of alluvial ridges and river avulsion. Earth Surf. Process. Landforms 43, 2409–2420. https://doi.org/10.1002/esp.4404.
Walling, D.E., He, Q., 1998. The spatial variability of overbank sedimentation on river floodplains. Geomorphology 24, 209–223. https://doi.org/10.1016/S0169-555X(98)00017-8.
Weissmann, G.S., Hartley, A.J., Nichols, G.J., Scuderi, L.A., Olson, M., Buehler, H., Banteah, R., 2010. Fluvial form in modern continental sedimentary basins: Distributive fluvial systems. Geology 38, 39–42. https://doi.org/10.1130/G30242.1.
Yuill, B.T., Khadka, A.K., Pereira, J., Allison, M.A., Meselhe, E.A., 2016. Morphodynamics of the erosional phase of crevasse-splay evolution and implications for river sediment diversion function. Geomorphology 259, 12–29. https://doi.org/10.1016/j.geo morph.2016.02.005.